"This report was prepared as an account of work sponsored by a Department of the Federal Government of Canada. Neither the Federal Government of Canada nor any agency thereof, nor any contractor or subcontractor, nor any of their employees, makes any warranty, expressed or implied, or assumes any legal liability or responsibility for any third party's use of or the results of any information, apparatus, product or process disclosed in this report, or represents that its use by such third party would not infringe privately owned rights".

A REPORT ON THE EVALUATION OF THE TWIN ARC NARROW GAP PROCESS FOR FIELD WELDING OF RAILS

BY

DR. PETER SOMSKY

WELDING INSTITUTE OF CANADA

Work on this project was conducted under the auspices of the Canada Centre for Mineral and Energy Technology, Energy, Mines and Resources, Canada.

FILE NUMBER:	007SQ.23440-8-9256
CONTACT SERIAL NUMBER:	23440-8-9256/01-SQ
CANMET PROJECT NUMBER:	
CANMET SCIENTIFIC AUTHORITY:	DR. R. CHANDEL

CONTRACT SERIAL NO. 89256-01-SQ
CONTRACT REQUISITION NO. 23440-8-9256
CONTRACTOR: WELDING INSTITUTE OF CANADA

MICROMEDIA

DATE: JANUARY 1990

72 pp

TITLE: **A REPORT ON THE EVALUATION OF TWIN ARC NARROW GAP PROCESS FOR FIELD WELDING OF RAILS**

FINAL REPORT

BY

DR. PETER SOMSKY

WELDING INSTITUTE OF CANADA

Work on the project was conducted under the auspices of the Canada Centre for Mineral and Energy Technology, Energy, Mines and Resources Canada.

FILE NO:	007SQ.23440-8-9256
CONTRACT SERIAL NO:	23440-8-9256/01-SQ
CANMET PROJECT NO:	
CANMET SCIENTIFIC AUTHORITY:	DR. R. CHANDEL

DATE: JANUARY 1990

91-04677/

Executive Summary

The Welding Institute of Canada has successfully designed, built, and tested a new system for welding rail steel. This system is based on a twin arc pulsed narrow gap gas metal arc welding process (Twin arc pulsed GMA-NGW). The welding procedures were optimized and a variety of rail steels and welding wires tested.

The results show that this system produces welds with higher mechanical strength, fewer defects, and has the potential for greater reliability than THERMIT welds.

This is the final report for Phase 1 and includes the major results from the first six milestones. A Phase 2 project should be initiated to test weld quality produced in field conditions.

Sommaire

L'Institut de Soudage du Canada a réalisé avec succès la conception, la fabrication et les essais d'un nouveau système de soudage des rails en acier. Ce système met en oeuvre le soudage pulsé à arcs jumelés sous gaz sur préparations étroites (procédé GMA-NGW pulsé à arcs jumelés). Les modes opératoires de soudage optimaux ont été recherchés et différents rails en acier et fils-électrodes de soudage ont été testés.

Les résultats obtenus montrent que ce sytème produit des soudures ayant une résistance mécanique plus élevée et moins de défauts et il permet d'escompter une plus grande fiabilité des soudures par rapport à celles obtenues par ALUMINOTHERMIE.

Ceci constitue le dernier rapport de la phase 1; il comprend les principaux résultats obtenus à chacune des six étapes du projet. La phase 2 devrait être engagée pour tester la qualité des joints soudés sur chantier.

Table of Contents

		Page
1.0	Introduction	1
2.0	Background	2
	2.1 The WIC Twin Wire Pulsed GMAW Process	
	2.2 Process Performance Criteria	
	2.3 Equipment Design Criteria	
3.0	Objective	3
4.0	Experimental Work	3
	4.1 Design of Welding Head and Chill Block Backing System	
	4.2 Functional Testing of the Welding Head and Backing	
	4.2.1 Testing of Welding Head	
	4.2.2 Testing of Weld Backing	
5.0	Installation of Computer Programmed X-Y Cross Slide Assembly	6
6.0	Determination of Optimum Welding Procedures	7
	6.1 Welding Rails	
	6.2 Welding Consumables	
	6.3 Optimization of Welding Procedures	
	6.3.1 Limiting Factors	
	6.3.2 Welding Current	
	6.3.3 Welding Voltage	

Table of Contents
(con't)

			Page
	6.3.4	Feed Speed	
6.4	Welding Head Manipulation		
6.5	Rail Set Up		
6.6	Optimum Welding Conditions		
7.0	Examination of Rail Welds		10
7.1	Metallographic Examination		
	7.1.1	Macro Examination	
	7.1.2	Micro Examination	
	7.1.2.1	Rail Metal	
	7.1.2.2	Weld Metal	
	7.1.2.3	Fusion Line	
7.2	Hardness Measurement		
7.3	Weld Tensile Strength		
7.4	Slow Bend Test		
7.5	Rail Weld Fracture Analysis		
	7.5.1	Rail Base in Tension	
	7.5.2	Rail Head in Tension	
8.0	Discussion		13
8.1	Welding Equipment Design		
	8.1.1	Power Source	
	8.1.2	Welding Head	

Table of Contents
(con't)

Page

8.1.3 Weld Backing

8.2 Welding Head Manipulation

8.3 Chill Block Backing System

8.4 Weld

8.4.1 Weld Metallurgy

8.4.2 Mechanical Properties

9.0 Conclusions 17

10.0 Recommendation 18

11.0 Acknowledgement 18

12.0 References 19

List of Figures

Figure 1	Basic set up for the twin wire process
Figure 2	Basic concept of the welding head design
Figure 3	Refined welding head with nozzle attachment for effective gas shielding
Figure 4	General view of the chill block assembly (photo)
Figure 5	A general view of X-Y cross slide assembly with wire feeders (photo)
Figure 6	Factors and parameters influencing the weed quality
Figure 7	Welding voltage versus time
Figure 8	Pattern of the head motion
Figure 9	Longitudinal section of the weld showing layers of the deposited materials
Figure 10	Rail set-up before welding
Figure 11	Appearance of the finished weld
Figure 12	Cross section of the non-stop rail weld (#080)
Figure 13	Cross section of the non-stop defect free weld (#086)
Figure 14	Cross section of the rail base parallel with the base (#070)
Figure 15	Cross section in the rail head parallel with the base (#085) showing hot cracks
Figure 16	Fine structure in a rail base (#078)
Figure 17	Columnar structure in a rail weld (#080)
Figure 18	Perlitic structure of the rail base (#078)
Figure 19	Weld metal microstructure from the upper part of the weld (#078)

List of Figures
cont'd

Figure 20 Weld metal microstructure after higher magnification (#078)

Figure 21 Weld metal microstructure (#081)

Figure 22 Fusion line between rail and weld metal in an upper portion of the weld (#078)

Figure 23 Fusion line between rail and weld material in a rail base (#078)

Figure 24 Fusion line between rail and weld metal in an upper portion of the weld (#081)

Figure 25 Hardness profile rail (#073)

Figure 26 Hardness profile rail (#080)

Figure 27 Hardness profile rail (#081)

Figure 28 Metric round tensile specimen

Figure 29 Fracture surface in a tensile specimen

Figure 30 Welded rail sections before bend testing

Figure 31 Fracture surface after bend test (#082)

Figure 32 Fracture surface after bend test (#076)

Figure 33 Fracture surface after bend test with non-typical character (#074)

Figure 34 Fracture surface after bend test with highest deflection (#083)

Figure 35 Fracture after bend test showing course surface in rail weld metal (#077)

Figure 36 Fracture after bend test showing course surface in most of the rail weld metal (#079)

Figure 37 Fracture after bend test demonstrating propagation from the HAZ in the rail head (#084)

List of Tables

Table 1 Optimum Welding Conditions

Table 2 Rail Welds Identification and Summary of the Testing and Welding Matrix

Table 3 Tensile Test Report

Table 4 Slow Bend Test Report

List of Appendices

Appendix 1 Wire ER 100 S-1

Appendix 2 Wire ER 120 S-1

A REPORT ON THE EVALUATION OF

THE TWIN ARC NARROW GAP PROCESS

FOR FIELD WELDING OF RAILS

Welding Institute of Canada Final Report RC350/10/90

Prepared for: **Department of Supply and Services Canada**

1.0 Introduction

Long welded rails (LWR) and continuously welded rails (CWR) have now spread worldwide. Although the cost of CWR is initially higher than that of conventional fish plated track, the savings in reduced maintenance costs, improved track stability, higher running speeds and lower power consumption provide an adequate return on capital, along with improved passenger comfort and greater safety.

Rail steels are now generally flash butt welded into transportation lengths of 200 to 300 m as LWR and then welded on site by the THERMIT process to produce the CWR system. The popularity of THERMIT welding process is due to; a) the initial cost of equipment and material is relatively low, b) portability allows on-site welding with no electric power or machines, c) it is claimed by consumable manufacturers that all commercially available rail steels are weldable.

The chief drawback of the THERMIT process is that the weld metal solidifies as coarse-grained pearlite in an "as-cast structure" conducive to low notch toughness. Coarse-grained structure is also formed in the HAZ of the parent rail, having a grain size approaching that of the weld metal. Extending out from the course-grained region is a soft annealed area with finer grains found at a distance of 50-60 mm (1.97 - 2.36 in.) from the centre line of the weld, extending out from the course-grained region. This characteristic softening of the THERMIT gives insufficient strength to withstand high cyclical stress concentration. For these reasons the failure rate of THERMIT welds in service is high. A safety hazard exists during winter when moisture from snow contaminates the thermit charge to make the process very hazardous. Therefore, there is a need to develop an alternative welding process particularly for joining recently introduced heat sensitive rail steels.

2.0 Background

Narrow gap welding (NGW) has long been viewed as a very promising but complicated

welding technique offering high productivity and cost effectiveness. The low heat input of the NGW process enhances quality through reduced distortion and HAZ size.

Bead deposition in NGW is either one-pass-per layer (monopass) or two-passes-per layer (bipass). Single and double electrode arrangements are common.

Gas Metal Arc Welding (GMAW) was the first welding process utilized for NGW and still accounts for most of the applications. The popularity of GMAW is due to the fact that the arc can be easily monitored allowing feedback control, the groove is relatively narrow and the process gives good weld toughness. However, lack of side wall fusion, intensive spattering and magnetic arc blow still intimidate many potential users of GMA-NGW [1,2].

Examples of narrow gap GMA-NGW welding for rail applications are still relatively rare. However, a rail welding robot was developed in Japan by Nippon Kokan K.K. (NKK) in 1986, in order to improve the quality and efficiency of field welding applications. The robot uses the patented NKK GMAW process with a rotating arc [3].

2.1 The WIC Twin Wire Pulsed GMAW Process

The twin arc pulsed GMA welding system, has been developed [4] and recently patented by the Technology Division of the Welding Institute of Canada.

Two independent inverter type power sources provide current to the two consumable electrodes. The pulse current output from each supply is synchronized to ensure that the peak current levels do not occur simultaneously. One power supply acts as a master control and the other as a slave unit in which the pulse output is time delayed from the master. The result is an oscillation of the arc by electronic means. The two electrodes are angled in the groove towards the walls to promote side wall fusion. The spacing of the electrode tips allows operation in gaps of 10 - 20 mm (0.4 - 0.8 ins.).

At the heart of the system is the patented power source design. This design utilizes arc voltage feedback signals to control the average welding current by instantaneously modulating the frequency of th current pulses. Thus high arc stability and welds of consistent quality are achieved.

2.2 Process Performance Criteria

The long term objective of this work is to develop a GMA-NGW system with the following advantages over THERMIT welding:

a) higher strength, wear resistance and fatigue life of the rail weld

b) narrower heat affected zone with elimination of rail softening

c) hardness profile in weld metal and HAZ close to that of the parent rail

d) lower reject rate in production welding

e) lower service failure rates

f) equivalent or higher productivity

g) lower cost per weld

2.3 Equipment Design Criteria

The long term objective is that the equipment:

a) be mechanized with significant computer/micro-processor control features

b) be compatible with minimum joint preparation on the rail ends

c) operate within an ambient temperature range of -28°C to +38°C (-20°F to +100°F)

d) incorporate improved safety features

e) cause minimal environmental pollution

3.0 Objective

The overall project objective was to adapt the WIC twin arc pulsed GMA-NGW process to the welding of full rail sections end to end. This objective was achieved in a number of steps as follows:

1) A special welding head was designed to give access to the bottom of the rail joint with an approximately 17 mm (0.67 ins.) gap between the rail ends.

2) A programmable X-Y cross slide assembly traversed the welding head back and forth in a path that progressively and continuously deposited weld metal across the rail base up the vertical web and across the head of the rail cross section.

3) A specially designed water cooled copper chill block assembly progressively supported the molten weld metal as the weld pool moved up the rail section.

4) Modification of the existing dual power Welding Source developed and patented by WIC.

4.0 Experimental Work

4.1 Design of Welding Head and Chill Block Backing System

This rail welding project was the first industrial application of this process in a "deep narrow

gap". For the welding head design the basic requirement was that the two contact tips had to direct wires against the side walls in the gap between the two rails. Moreover, the head design had to completely shield the molten metal against oxidation. From previous experiments the wires were configured as shown in Figure 1.

More specific requirements on the head design are detailed below:

1) The width of the welding head had to be minimal (13 mm).

2) The welding head had to reach to the bottom of the rail of maximum height 187mm. (The requirement was actually set at 200 mm to provide for clearances).

3) The head had to carry an average welding current of 200A at 100% duty cycle.

4) The head had to be liquid cooled to ensure a sufficiently low working temperature of the contact tips and nozzle.

5) The head had to accommodate both 0.9 mm (0.035 in.) and 1.2 mm (0.045 in.) diameter wire.

6) The two contact tips had to be electrically insulated.

7) The head had to be mechanically strong.

8) The head had to perform in both travel directions, moving back and forth during welding.

9) The head had to perform in both the deep root passes and on the capping passes as well. This dual requirement was very difficult to fulfil. None of the commercially available narrow gap head designs, which was satisfactory for the root pass, could also perform the capping passes.

The design of the head involved several components including a unique gas shielding system. The importance of a good shielding was recognized at the outset, therefore, an effective triple shielding system was decided upon. Its main gas supply used a ceramic tube positioned in the centre of the head. The straight shape and smooth inside surface guaranteed laminar gas flow and good coverage of the weld pool area. This ceramic tube also electrically isolated the two symmetric conductive components of the head. Supporting side shields were attached to the head to direct the shielding gas. Water cooling through the head was provided for the contact tips to prolong their service life. All electrically conductive parts of the head were made from copper, for high thermal and electric conductivity and good machinability. Figure 2 illustrates the basic welding head design and the shielding system.

The main function of the chill blocks was to cool the rails. The cooling capacity had to be high enough to prevent fusion between the molten weld metal and the chill blocks. Also, it was very important that the chill blocks were in close physical contact with the rails to ensure efficient heat transfer from the rails to the blocks. The next requirement was to support the

molten metal from the sides for one specific rail size; 136 lbs/yd according to American Rail road Engineering Association (AREA). The final requirement was that the blocks had to be open on the sides above the pool surface during welding to enable the welding head to travel back and forth across the rails.

Two alternative designs for the backing system were drawn:

a) a simple manually operated design consisting of seven segments

b) a complicated automatically operated design consisting of 21 segments and 10 air cylinders

Since financial resources for the project were limited the much cheaper manual design was chosen. This choice of a simple design facilitated build-up to more complex systems in Phase 2 through the addition of new components. It was foreseen that solidification of the molten metal would in initial tests be supported from both sides by small copper blocks slid in from the sides manually.

4.2 Functional Testing of Welding Head and Backing

4.2.1 Testing of Welding Head

The first welding head design was initially tested by moving back and forth between 50 mm (1.97 in.) thick plates in a 12 mm (0.47 in.) gap. A shielding gas mixture of 90% Ar + 10% CO_2 was used. Gas flow in the central tube was independent of the side tubes so that the two different flow rates could be adjusted. Various flow rates in the central and side tubes were tried but none of these adequately shielded the weld. Heat generated during welding, particularly when reversing the travel direction, caused uncontrolled turbulence, therefore arcing between the contact tips and side walls (so called melt down). Therefore, a new approach with a nozzle attachment was tried. It was clear that this attachment would increase the thickness of the welding head and draw off excess heat. Another technical problem was the necessity to insulate the nozzle electrically from the contact tips. Two alternatives seemed to work - a copper nozzle with ceramic insulation or a one-piece custom made ceramic nozzle. A market survey for custom made ceramic nozzles revealed that they cost around $900 each which was excessive for our budget. Therefore the welding head was modified by a unique liquid cooled copper nozzle made in-house as illustrated in Figure 3.

Continued testing confirmed that the adapted head provided satisfactory shielding gas coverage, both at the root of the weld and for the capping passes.

The shielding was adequately efficient and a successful capping pass could be deposited at a travel speed as high as 0.5 m/min (20 in./min). It was subsequently demonstrated that the head could perform between 50 mm (1.97 in.) thick plates thus the trials using rails instead of plates were started.

4.2.2 Testing of Weld Backing

The chill block backing system is illustrated in Figure 4. The cooling water flow rate was set at 10 l/min (~2.5 gal/min) which proved to be satisfactory.

Special attention was devoted to the horizontal and vertical rail alignment in the range ±1.0 mm (0.04 in.). Due to weld metal shrinkage the initial gap was set at 17 mm (0.67 in.) at the rail base and 20 mm (0.79 in.) at the rail head.

Two challenges had to be met, the first was welding of the rail base. Most previous attempts by researchers experimenting with all known arc welding processes could not deliver sufficient heat input while maintaining a stable arc. The second task was to keep the rest of the rail profile free of typical weld defects such as lack of fusion and porosity.

Three alternative backings for the welding of the rail base were tested:

a) Welding onto a steel backing was successful. The first pass established a consistent arc and generated sufficient heat for good sidewall fusion at the rail base. It was interesting to note that the heat build-up and dilution increased as welding progressed. This was a strong indication of the need for heat input control which should be pre-programmed, maximized at the base, minimized at the web and the rail head.

b) Welding onto a copper backing was not successful because too much heat accumulated in the copper. This caused the copper surface to fuse with the weld deposit. Even intensive water cooling of the copper backing did not prevent this undesirable fusion.

c) Welding onto a copper backing overlaid with a consumable steel strip was also not feasible. Trials with strips 4.8 (0.19 in.), 1.8 (0.07 in.) and 1.5 mm (0.06 in.) thick failed to produce acceptable fusion between the rails and strips.

5.0 Installation of Computer Programmed X-Y Cross Slide Assembly

To facilitate the X-Y cross slide installation two subassemblies had to be designed and machined, a base plate with triangular reinforcement and a welding head holder. Both units were made from aluminum plate and fitted into the X-Y cross slide assembly. The X-Y cross slide assembly was then mounted on a special steel frame.

A separate stand-alone square tube arm with two wire feeders and wire spools also sat on top of the table (Figure 5). The arm carried the weight of all electric cables and hoses so the load on the welding head was kept to a minimum. There were three control boxes fixed to the arm; two wire feed controllers and one slide controller. This arrangement was convenient and enabled the operator to control the welding process with one hand while observing the progress.

The slide controller directed the entire drive electronics through an interface card on instructions from a personal computer with battery back-up. The software for the PC enabled it to accept and transfer a program for motion control. Pre-programmed values gave very accurate positioning of the cross slides by stepping motors, which drove the slides and

controlled their acceleration and deceleration ramping.

The slides performed very well during head manipulation. They were extremely sturdy, precise and repeatability in positioning came to within 0.025 mm (0.001 in.).

The main disadvantage of the cross slide assembly described lay in its off-line programming. Since the assembly was activated by start-stop-reset knobs, advanced control of the welding head while welding was in progress was not possible. Occasionally the welding had to be stopped due to a malfunction, and the welding head moved out, checked, moved in again and welding resumed.

6.0 Determination of Optimum Welding Procedures

6.1 Welding Rails

Two group sponsors, Canadian National (CN) and Algoma, were approached to deliver AREA [1] 136 lbs/yd rails for testing as this grade of rail is the most common. Canadian National supplied a standard grade manufactured by Sydney Steel. The exact chemical composition of this particular steel is not known, but the AREA specification requires 0.69-0.82% C, 0.10-0.25% Si and 0.70-1.0% Mn, with a tensile strength of approximately 800 MPa.

Algoma supplied alloyed rails with 0.75-0.82% C, 0.3-0.5% Si, 0.85-1.10% Mn, 1.25-1.30% Cr and 0.05-0.11% V, with a tensile strength of approximately 1000 MPa.

6.2 Welding Consumables

Three grades of filler wires were used:

a) A standard deoxidized wire conforming to AWS/SFA5.18 class ER70-S6 with a 0.9 mm (0.035 in.) diameter was used. The chemical composition of this wire was 0.07-0.15%C, 1.40-1.85%Mn, 0.8-1.15%Si and the as-welded tensile strength was ≥ 500 MPa.

b) A low alloy Ni, Mo, Cr wire from Thyssen A.G, conforming to AWS A5.28 class ER100-S1 with a diameter of 1 mm (0.039 in.) was used. The chemical composition of the wire and mechanical properties of the weld metal are given in Appendix 1. The as welded tensile strength was ≥740 MPa.

c) A low alloy wire from L-Tec conforming to AWS A5.28 class ER120-S1 was used. The chemical composition of the wire is given in Appendix 2. The as-welded tensile strength should be close to 1000 MPa.

6.3 Optimization of Welding Procedure

The basic objective was to optimize all factors influencing the quality of the rail welds. The way in which all the factors were interrelated is illustrated in Figure 6. Altogether, fifteen

parameters had to be adjusted to give optimum weld quality. Most of these were interdependent and this made optimization a challenging and time consuming task.

6.3.1 Limiting Factors

There were some factors which were preset by the design including the welding gap, average current, gas shielding, tips, and stand-off distance. These limiting factors are discussed below:

a) The welding gap was governed by the width of the head which was set at 13 mm (0.51 in.). The minimum gap was 17 mm (0.67 in.) to ensure enough clearance for head motion. Although the rails were restrained, the closing of the gap as a result of weld shrinkage became greater as more fill passes were deposited. Therefore, the gap was set at 17 mm (0.67 in.) at the rail bottom and 20 mm (0.79 in.) at the rail head.

b) The power source for the twin arc pulsed GMA-NGW was originally custom built for 60% duty factor and an average current of 200A. The actual duty cycle when non-stop rail welding was 100% therefore, the maximum average current had to eventually be decreased to 160A to avoid overheating the machine.

c) Gas shielding using a 90%Ar+10%CO_2 mixture was sufficient at a flow rate of 15 CFH on the centreline and 30 CFM on the sides. This gas coverage produced sound weld metal free of porosity at the rail bottom and the rail head which would both have been unforgiving to inadequate shielding.

d) The typical contact tip outside diameter was 5.5 mm (0.22 in.) and the length 72 mm. (2.84 in.) The inside diameter of 1.2 mm (0.045 in.) provided the longest life for the wires used. The contact tips after being screwed into the welding head were bent to conform to the configuration illustrated in Figure 1.

6.3.2 Welding Current

The limitation on the current output of the power source discussed above led to the following settings:

a) the peak current output was set at 280A on the master and 300A on the slave

b) the background current was set at 40A (master) and 50A (slave)

6.3.3 Welding Voltage

The average welding voltage for the master and slave outputs is seen in Figure 7. The values were more or less stabilized except for the lifting points. The low voltage (25V) produced a shorter and more digging arc (~3 mm) while the higher voltage (27V) produced a longer and softer arc (~6 mm).

6.3.4 Feed Speed

The wire feed speed was another one of the interdependent factors. Speeds close to 8.89 m/min (350 in/min) produced high arc stability and extended contact tip life.

6.4 Welding Head Manipulation

The head manipulation was crucial to the weld quality, especially the fusion characteristics. In all tests, the head was positioned in the centreline of the weld and moved in the "X" axis (travel) and "Y" axis (lift) directions.

The optimal travel speeds supplied good sidewall melting. At too low travel speeds, molten metal rolled in front of the arc and this hampered proper sidewall fusion. At too high travel speeds there was insufficient heat input. The optimum travel speed was selected around 127 mm/min (5 in. min).

The optimum lifting distance per pass was dependent on the amount of melted wire at 8.89 mm/min 8.89 (350 in. min) and the gap 17 mm (0.067 in.). A lift of 3 mm (0.12 in.) after every transverse motion maintained the required stand off distance of 15 mm (0.59 in.).

The pattern of the head motion was rectangular (Figure 8). However, the travel speed was different inside and outside the actual rail profile. The travel speed was decreased by approximately 35% outside the rail profile to compensate for the wider gap between the copper chill blocks (20 mm) than between the rails (17 mm). When this compensation was not made, the layers were not deposited in a constant horizontal level and so the tip to work distance changed from the centre line to the lift up points (Figure 9).

The frequency modulated power source responded positively to the arc length changes at the lift points in less than one second. However, too long a stick out after the lift caused arc instability. Hence, automatic stick out control should be an essential part of the welding head manipulation in any future design.

6.5 Rail Setup

The rails were placed in a simple jig and clamped mechanically (Figure 10). Firm clamping was necessary to prevent the initial gap of 17 mm from closing to less than 15 mm by the time welding reached the upper rail position.

It was recognized that welding at start-up onto cold metal would be crucial for the weld properties, particularly since only a limited heat input was available. In order to build up enough heat prior to welding at the rail base, three measures were taken; the first was a preheat to 100°C, the second a groove in the backing bar (Figure 10a, b) and the third was a combination of both.

6.6 Optimum Welding Conditions

The welding conditions summarized in Table 1 may be considered as optimum. The total

welding time non-stop was 35 minutes. The appearance of the finished weld is shown in Figure 11.

7.0 Examination of Rail Welds

The rails were successfully welded after resolving problems associated with the power source. Table 2 shows rail weld identifications and summarizes the welding and testing matrix.

7.1 Metallographic Examination

7.1.1 Macro Examination

A number of welds were cross sectioned at the centre of the rail to detect defects from top to bottom. The critical location was the rail base where lack of fusion (LOF) defects occurred (Figure 12).

The width of the HAZ reflected a rough balance between the heat generated by the power source and the heat conducted away through the joint. Heat conduction dominated during welding of the cold base which produced a narrow HAZ, the heat flow and HAZ width stabilized. Later on heat conduction into the rail head was high which caused the HAZ to get narrow again. The HAZ widened when the heat was accumulated in the upper part of the rail head.

A defect free weld is shown in Figure 13. The unique weld metal deposition pattern of the twin wire setup is visible throughout the weld, shows arcing close to the sidewalls.

A cross section of a rail weld cut parallel to the base on a weld made with an ER 70-S6 wire is shown in Figure 14. The fusion line is clean and no visible defects were detected in the weld metal. However, some sections welded with ER 120-S1 wire showed hot cracks, particularly in the rail head (Figure 15) where heat was accumulated.

The grain structure of the weld deposit appeared to be highly refined in the rail base as a result of repeated recrystallization followed by fast cooling during subsequent passes (Figure 16). However, the grain structure was changed over the web portions of rails, where temperature distribution stabilized and slower cooling rates took place. Here a columnar structure characterized the weld deposit to largely obscure individual passes (Figure 17). The dark spots in the HAZ appeared to be micro-cavities as will be shown later.

7.1.2 Micro-Examination

7.1.2.1 Rail Metal

The microstructure of the Sydney rail is shown in Figure 18. It is a typical perlitic structure. The microstructure of the Algoma rail was identical. The structure is consistent with a hardness of 290 - 310 HV 30.

7.1.2.2 Weld Metal

A typical weld metal microstructure from the upper part of the weld deposited by ER 70-S6 wire is seen in Figure 19. The metal has no alloying beyond a minimum amount of Mn and Si so it is essentially a carbon steel. Low magnification shows a fine equiaxed grain structure containing ferrite and pearlite as seen in Figure 20. At higher magnification (300x), a shrinkage micro-crack associated with the presence of inclusions is visible. The structure is consistent with the hardness 180 - 200 HV30.

A typical weld metal microstructure from the upper part of the weld deposit using ER 120 S-1 wire (Figure 21). The microstructural constituents include fine grained ferrite, aligned and non aligned ferrite with second phase including bainite and/or martensite. The fine grained ferrite consists of relatively small bainitic-ferrite packets which were responsible for the superior strength and increased hardness (270 -290 HV30). Also, a shrinkage micro-crack is visible.

7.1.2.3 Fusion Line

The temperature gradient from the fusion line into the HAZ and the chemistry of the parent metal establish the width of the HAZ and its microstructure. The coarse-grained region of the HAZ which borders the fusion line can be critical to the integrity of the joint. In particular the area of liquation cavities which typically form in the coarse-grained region varies with the HAZ width.

Figure 22 illustrates the HAZ in an upper portion of the rail weld. Typical liquation cavities are visible at the grain boundaries in the coarse-grained region. Propensity for grain boundary liquation seems to be related to sulphur and its tendency to diffuse into the grain boundary area at elevated temperature. The effect is seen in Figure 23. In spite of the higher magnification used (200 X), only small liquation cavities were detected in the same weld at the rail base where the temperature gradient was steeper and the HAZ narrower. Hence minimizing the width of the HAZ would seem to be important to suppress liquation cracking. Both rails were prone to liquation cavities. Figure 24 shows the presence of a liquation cavity in the Algoma rail.

7.2 Hardness Measurement

The macrohardness HV30, according to ASTM E 92-82, was measured on etched rail cross sections at three different levels (1, 2 and 3) in order to cover different widths of the HAZ. The levels measured from the rail head were located as follows: level 1 = 5 mm (0.2 in.); level 2 = 120 mm (4.72 in.) and level 3 = 180 mm (7.08 in.).

The measured values from most of the representative welds are graphically illustrated in Figures 25, 26 and 27. Although the ultimate goal was continuous welding, sometimes an interruption was necessary. In such a case, the HAZ was slightly modified and a minimum of three passes were required to restore the full width of the HAZ.

The base metal hardness for both the Sydney and Algoma rails ranged from 280 to 290

HV30. The weld metal hardness depended on the consumable wire. The highest hardness (250-280) was obtained as expected from ER 120 S-1. It is worth mentioning that this expensive consumable was developed for welding high tensile steels, specifically for HY100. The lowest hardness (160-180) were obtained from the relatively inexpensive consumable wire ER 70 S-6.

The maximum hardness in the HAZ (400-480) were always obtained in the rail head as the result of excessive heat accumulation and rapid cooling on completion of welding (level 1). The lowest hardness was obtained at level 3 where the small heat accumulation was followed by a rapid weld cooling and the hardness was equal to the base metal.

7.3 Weld Tensile Strength

Round tensile specimens as detailed in Figure 28 were machined from the rail weld. Two specimens (#5, 6) were taken from the rail web and three (#8, 9, 10) from the rail base. As indicated in the Tensile Test Report (Table 3), the ultimate tensile strength was above 100,000 psi except for #6. The fracture surface shown in Figure 29 verified the presence of shrinkage cracks in the weld metal as already analyzed in section 7.1.2.2.

7.4 Slow Bend Test

Eight welded rail sections shown in Figure 30 were submitted to the CN laboratory for standard slow bend testing. Some of the rails were tested with the base in tension and others with the head in tension.

The test results are summarized in Table 4. The scatter of maximum test loads indicates the presence of weld defects as can be seen on the fractured rail surfaces. A test load of over 400,000 psi with the rail base in tension is considered satisfactory, thus all tests either passed or were very close to passing.

7.5 Rail Weld Fracture Analysis

7.5.1 Rail Base in Tension

Weld rail 6 performed extremely well during the bend test (load 456,000 lbs, deflection 0.75 in.) as shown in Table 4. During testing two fractures developed as shown in Figure 31. One fracture was located close to the fusion line, initiated most probably by structural changes in the HAZ. The second fracture occurred in the rail base. Presumably this fracture was initiated by a notch in the parent metal. No portion of the fracture was observed in the weld metal, thus confirming the high quality of weld metal deposit.

Weld rail 3 also performed very well during the bend test (load 414,000 lbs., deflection 0.7 in.), although the rail was from a different manufacturer (Sydney) and a different wire (ER 70 S-6) was used. The fracture appearance (Figure 32) was very similar to the fracture in weld rail 6.

Weld rail 1 recorded the lowest values during the bend test (load 366,000 lbs., deflection 0.5 in.). It is not clear as why the fracture was 80% outside the HAZ as seen in Figure 33. The fracture may have initiated in the HAZ (rail base right hand corner) and propagated through a weak link in the rail base material.

Weld rail 7 recorded the highest deflection (1.05 in.) at a reasonable load of 390,000 lbs. The fracture initiated in the HAZ of the rail base and propagated into the rail as illustrated in Figure 34.

7.5.2 Rail Head in Tension

Weld rail 4 performed very well during the bend test (load 390,000 lbs., deflection 0.75"). The fracture initiated in the weld metal of the rail head as a result of a dendritic structure and the presence of shrinkage cavities as discussed in section 7.1.2.2. This weld metal fracture surface (Figure 35) had a very different character from the relatively smooth rail base metal.

Weld rail 5 performed less adequately during the bend test (load 348,000 lbs., deflection 0.45 in.) than weld rail 4 in spite of identical materials and welding parameters. The fracture surface is shown in Figure 36.

Weld rail 8 recorded the lowest values during the bend test (load 342,000 lbs., deflection 0.3 in.). The fracture, (Figure 37) appeared close to the fusion line in the HAZ. Apparently the strength and ductility of the weld metal deposited by ER 120 S-1 exceeded the properties in the HAZ [8]. The extensive structural degradation and the higher hardness in the HAZ as discussed in section 7.3 contributed to these poor results.

8.0 Discussion

This challenging project was basically a feasibility study of a completely new welding technique.

8.1 Welding Equipment Design

The WIC synchronized pulsed twin wire GMAW narrow gap technique is highly innovative and useful for the narrow-gap welding of rails. The process utilizes two wires arcing simultaneously so that the heat source is "expanded" and temperature in the gap is ideally distributed as illustrated in Figure 2. The maximum heat comes in at the side walls to suppress incomplete fusion while the minimum heat occurs at the weld centre line. The rail gap (17mm) can be filled without any head or wire oscillation at an average current as low as 160 A. For comparison, a single wire rotating arc NG process [9] required 300A in a comparable gap.

8.1.1 Power Source

The power source used for the twin arc process was custom built for a previous project [4]. In the course of the present work many adjustments, particularly the introduction of additional

cooling, were required. At the optimal setting (Table 1) the power source produced spatter free metal transfer due to special circuitry, so called frequency modulated, which maintained high degree of arc stability.

8.1.2 Welding Head

The welding head, after it was adopted by fitting on a special liquid cooled nozzle, was used for all rail welding, performed extremely well, and was found to have the following advantages over known designs:

a) The head is a compact, narrow (only 13mm wide), self contained and rigid unit.

b) The gas shielding is efficient and reliable. The triple gas shielding with the centrally located ceramic tube is a striking technical innovation. The gas flow pattern forms an insulation barrier preventing electric arcing between the head conducting components and the welded rail. No additional gas supply outside the head assembly is required.

c) The liquid cooling of the head, particularly that of the nozzle, is efficient and reliable. Components such as the nozzle and contact tips are easily replaceable for quick maintenance with a cooling water lock-out for added convenience.

d) The nozzle is electrically isolated, and occasional contact with the welded rail doesn't cause short circuits.

e) The head performs equally well deep in the gap or on capping passes.

f) The total gas flow rate is economical at 45 CFH.

Whereas this new head design incorporates its own shielding, most of the competing narrow gap head designs [1,2] require auxiliary gas shielding. The rotating arc for example [3] relies on additional gas shielding supplied through the chill blocks.

8.1.3 Weld Backing

Among the three backings tried for the root pass, the steel backing with a 2mm groove was found satisfactory.

8.2 Welding Head Manipulation

The welding head computer controlled movement as described in section 6.4 fully satisfied the project requirements. The application of the computer controlled slides was the first application of this type undertaken by WIC and effectively replaced a much more expensive welding robot. However for field welding applications a more sophisticated head manipulation with automatic functions will be required. The "X" axis (travel) will have a program value and digital velocity feedback. The "Y" axis (lift) will have an adaptive, through the arc proximity control subsystem, which will maintain the desired position of the welding head over the molten pool. A new axis will have to be introduced to control the position of the

head inside the gap. Certainly head oscillation is foreseen for a wider gap.

8.3 Chill Block System

The manually operated chill block system basically forms the rail profile and conducts away the heat generated during welding. The present chill block design had the following features:

a) The rails could be vertically or horizontally offset or even worn down as the most rails in the field are.

b) Open sides in the chill block assembly allowed unrestricted gas flow free of turbulence which is unknown in enclosed chill block systems. The GMA-NGW rail welding robot [3] is the only one currently known, uses a completely closed chill block system so the arc shielding is very problematic.

c) Good visibility from the sides permits excellent process control.

8.4 Weld

8.4.1 Weld Metallurgy

As described in section 7.2, during rail welding at the base the deposit had rapid solidification of the weld metal and high cooling rates, whereas later on during the rail head welding the metal was deposited with elevated interpass temperatures. Here the low cooling rates contributed to a large weld pool and hot cracking (Figure 15).

Hot cracking occurs whenever sufficient stress is applied to a susceptible microstructure. In the present case, two types of cracks were observed; solidification cracks in the weld metal and liquation cracks in the rail base metal. Metallurgical factors that promote hot cracking are mostly low melting constituents in base metal such as sulphur, phosphorus, as well as presence of oxygen [9]. Hot cracking sensitivity (HCS) may be evaluated by various formulae. For example the HCS calculated by Houldcroft gave 19.46 for Sydney rail and 16.1 for Algoma rail. The value for non-sensitive steel should be less than 4. Hence it is evident that these rail steels are highly susceptible to hot cracking.

Weld metal is specifically designed to resist cracking. However, during welding it is diluted with the molten rail steel and particularly where substantial heat has accumulated in the joint. Actually hot cracking was not observed at the rail base but very frequently at the rail head. Therefore, controlled heat input with modified interpass temperature control should aim to give maximum heat input and minimum cooling at the rail base and the opposite at the rail head. This heat control should be an important feature in any rail welding exercise.

The success of rail welding depends considerably upon the weldability of the rail steel available. Among the most significant changes in railmaking technology introduced recently is the application of the continuous casting process. The faster and more uniform cooling rates which occur during solidification as compared to traditional ingot production greatly

reduce macrosegregation. Also refinement in steelmaking has brought cleaner steels. However rail welding with an intensive localized heat of the welding arc still faces hot cracking phenomena even with the most advanced rail steels.

In general it may be concluded that hot cracking has been observed but the specific composition ranges and welding conditions through which elements act to promote or inhibit such cracking are still to be determined.

8.4.2 Mechanical Properties

Slow bend test results, which are the most important for rail weld evaluation, are shown in Table 4. Those results are comparable with published Japanese data [3], (max. load 388,000 lbs. base in tension, and 348,324 lbs. head in tension). THERMIT welds have approximately 20% lower and flash butt welds 10% higher slow bend test values [10] in comparison with the present welds. However flash butt welding cannot be used in the field.

Mechanical values depend largely on the presence of weld defects. Lack of fusion defects were not observed frequently in this project. Once the welding process was optimized no major defects, except hot cracks, were detected. Heat treatment of rail welds, according to a Japanese source, would improve slow bend test results.

9.0 Conclusions

The following conclusions can be summarized:

1) New Twin Arc Pulsed Narrow Gap technique, based on the patented WIC principle, has been developed and applied for rail welding.

2) A conceptually new, innovative designed, lightweight and compact, liquid cooled twin wire welding head has been developed and tested.

3) A high precision computer controlled two axis head manipulation system has been successfully developed for rail welding.

4) The Twin Arc Synchronized Pulsed Frequency Modulated Narrow Gap GMA- has demonstrated a high potential for field welding of rails.

5) An optimum procedure for rail welding has been established. The gap was 17mm, diameter of welding wire 0.9mm (0.035 in.), average current 160A, average voltage 26V, total welding time 35min., preheat temperature 100°C/10min.

6) The mechanical properties of the twin wire rail joints are very promising. The slow bend test results for comparable rail steel are approximately 20% higher than THERMIT welds. The weld metal deposit by ER 120 S-1 wires has the required strength and hardness to meet the demand of the railway industry.

10.0 Recommendation

It is a prime objective of this rail welding program that it lead to the development of commercial technology.

One of the Group Sponsor Partners Holland has already separately contracted out to Kinetic Energy Corporation (KEC) for the development of a commercial prototype of a welding robot, based on the WIC approach. The development of this robot is already at an advanced stage.

There is continuing interest on the part of the other Group Sponsor (CN Rail, Algoma and WIC) to perform in depth evaluations of rail welds produced in the field by the KEC robot as Phase 2. Therefore the continuation of the program as Phase 2 is strongly recommended.

11.0 Acknowledgement

The Welding Institute of Canada and the author would like to express gratitude to the sponsors, namely The Federal Government of Canada (DSS and CANMET), Holland Company, Canadian National, and Algoma Steel.

12.0 References

1) Narrow Gap Welding
"The state-of-the-art in Japan"
Technical Commission on Welding Processes
The Japan Welding Society 1986

2) Malin V.
Monograph on Narrow-Gap Welding Technology
Welding Research Council, Bulletin 323, May 1987

3) Nohura H., Sato Y, Nishi Y.:
"Development of an Arc Welding Robot for Site Weldings of Rails",
Nippon Kokan K.K. Report Abstract 10146 (May 1986)

4) Ditschun A., Zajaczkowski B.:
"Twin Arc Pulsed GMA Welding"
WIC, RC233, September 1987

5) Ditschun A., Eaton N.F., Lassaline E., Zajaczkowski B.:
"The Development and Application of a Synchronized Twin Arc Frequency Modulated Pulsed GMAW/MIG Welding System." IIW DOC. XII-1067-88

6) Somsky P.:
"Milestone Report on the Evaluation of the Twin Arc Narrow Gap Process for Field Welding of Rails", WIC, RC350,(Milestones 1 to 4)
November 1989

7) Somsky P.:
Milestone Report (Milestone 5)
WIC RC 350/2, March 1990

8) Somsky P.:
Milestone Report (Milestone 6)
WIC RC 350/7 August 1990

9) Goodwin G.M.:
"Hot Crackings: Measurement, Mechanisms and Modelling"
Welding Journal, February 90, p. 26-31

10) "Rail Steels - Developments, Processing and Use" ASTM 1976

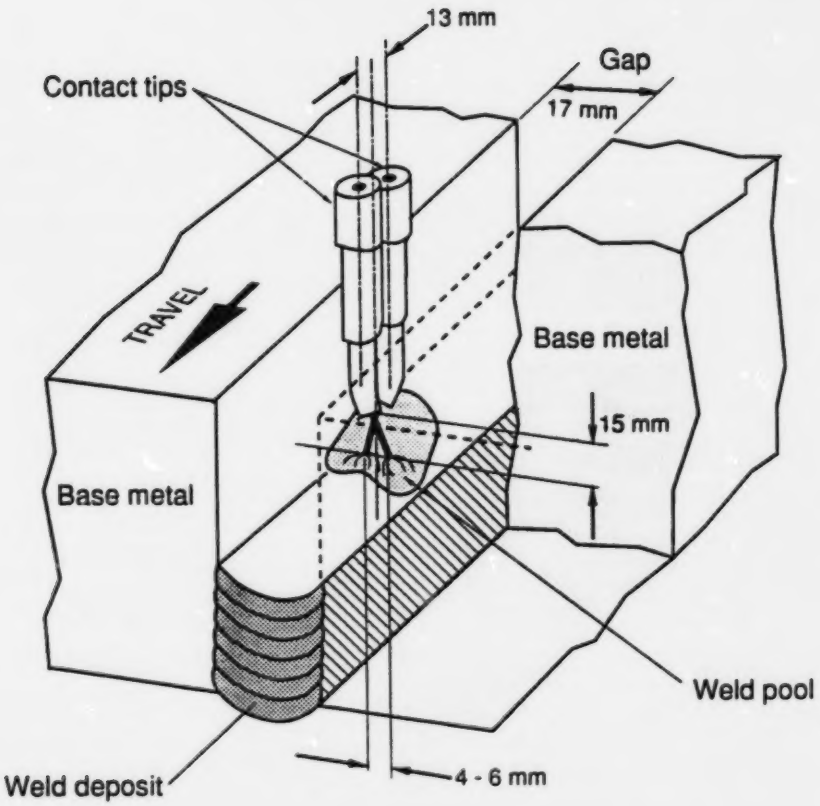

Figure 1. Basic setup for twin wire process.

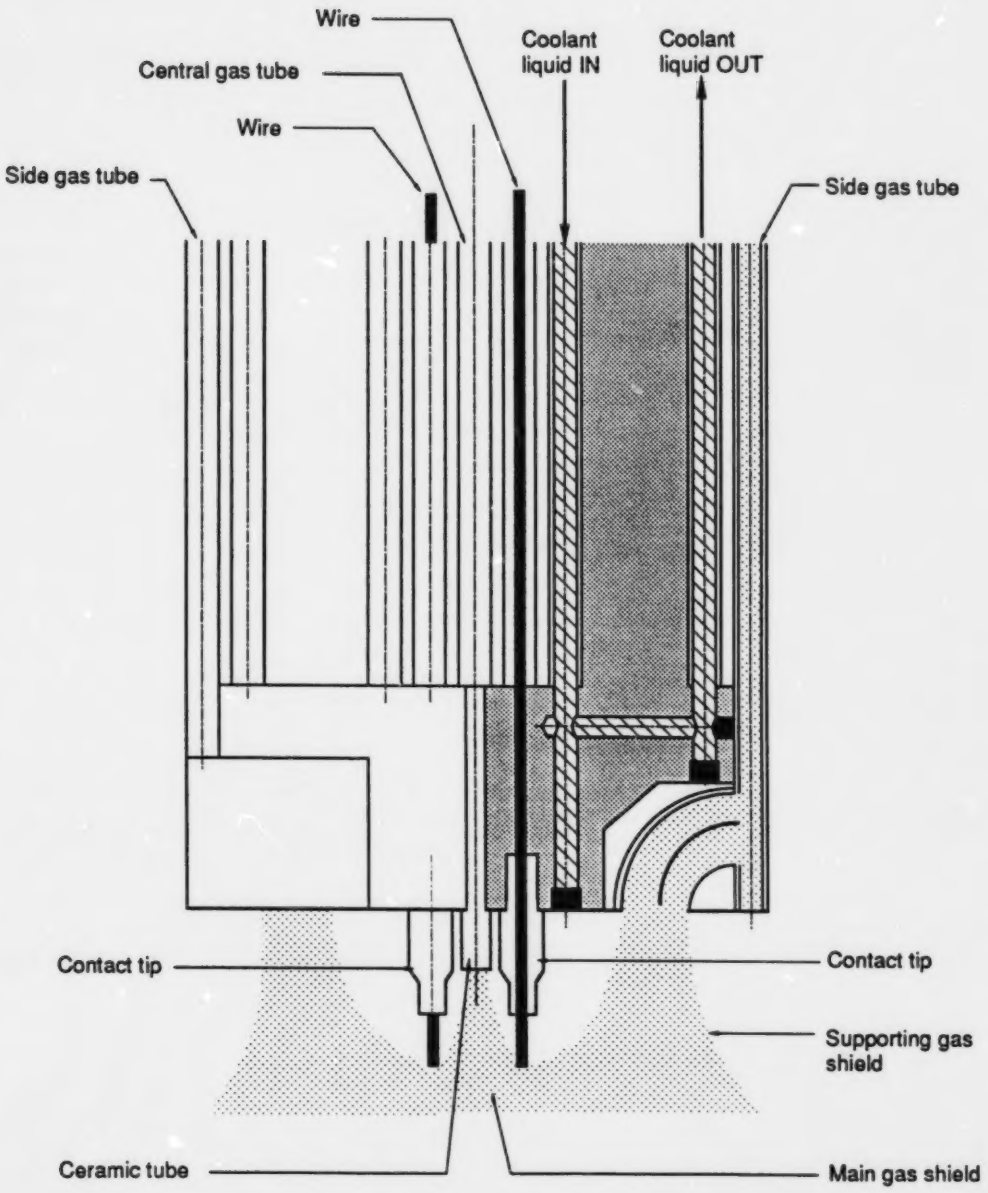

Figure 2. Basic concept of welding head design. Schematic of triple gas shielding.

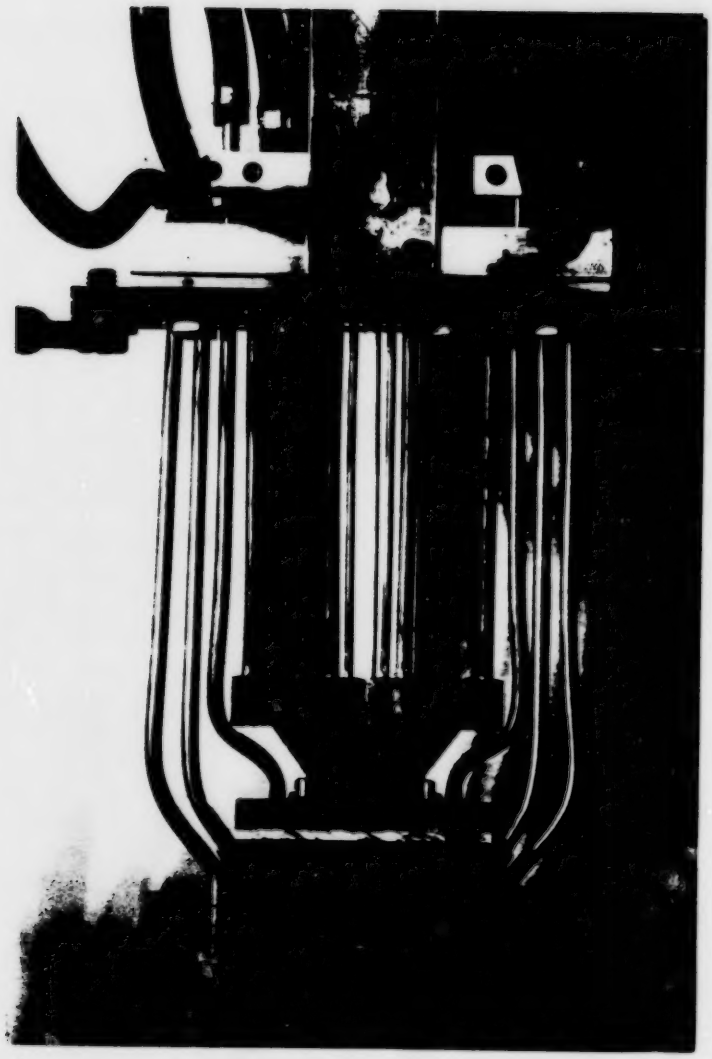

Figure 3. Refined welding head with the nozzle attachment for effective gas shielding. Nozzle is liquid cooled.

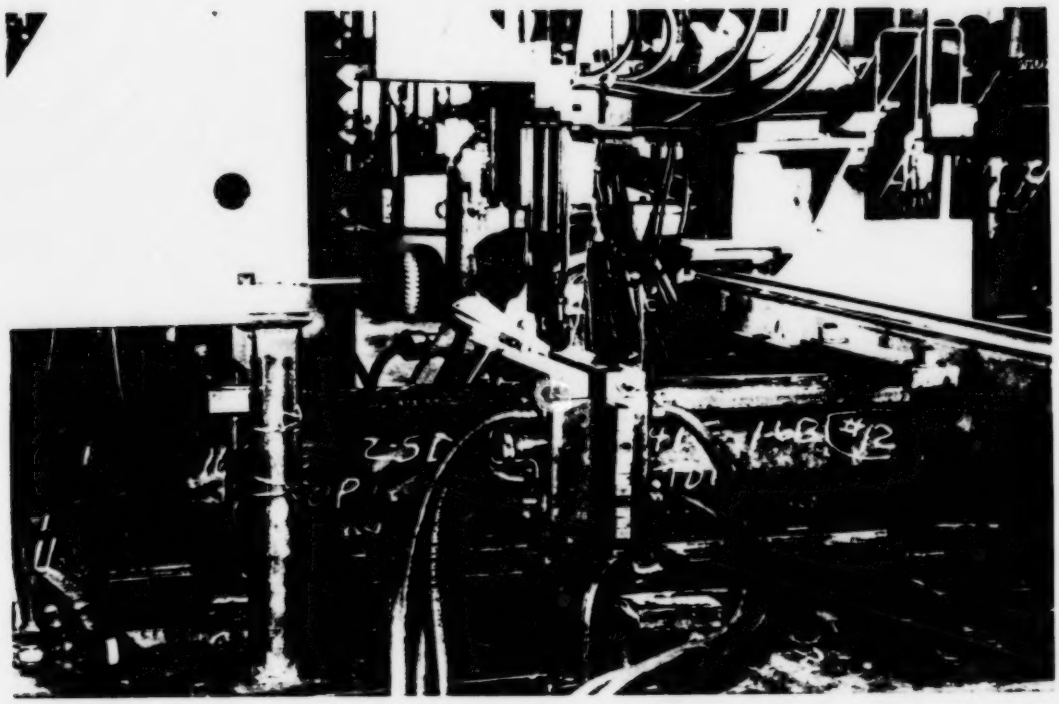

Figure 4. General view of the chill block assembly.

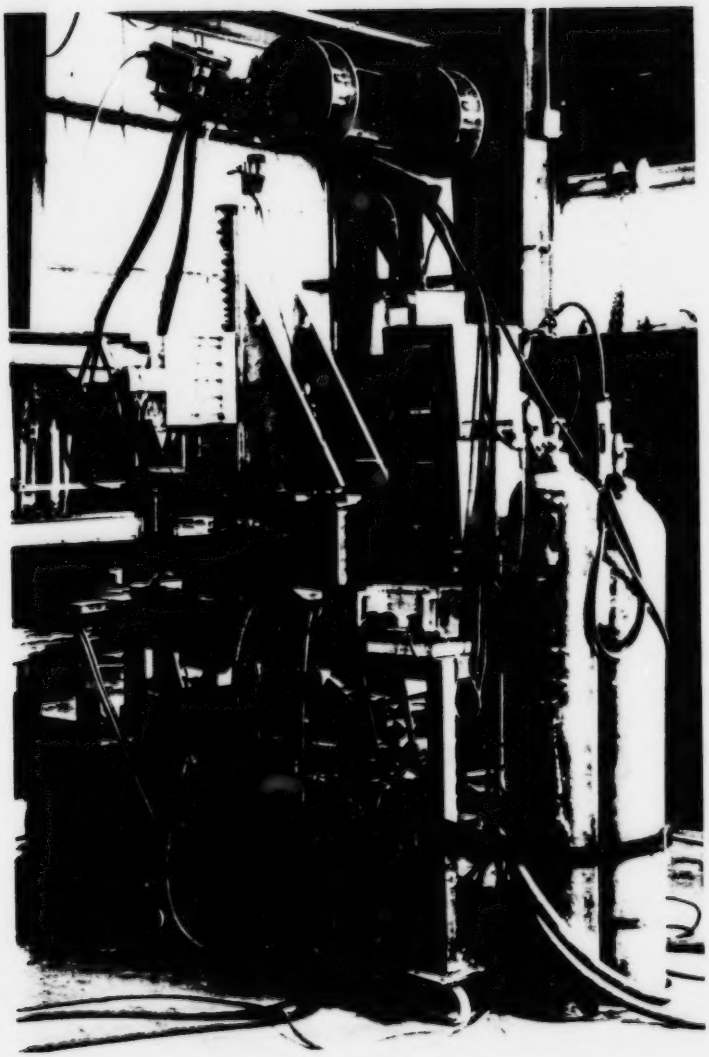

Figure 5. A general view of X-Y cross slide assembly with feeders.

Figure 6. Factors and parameters influencing the weld quality.

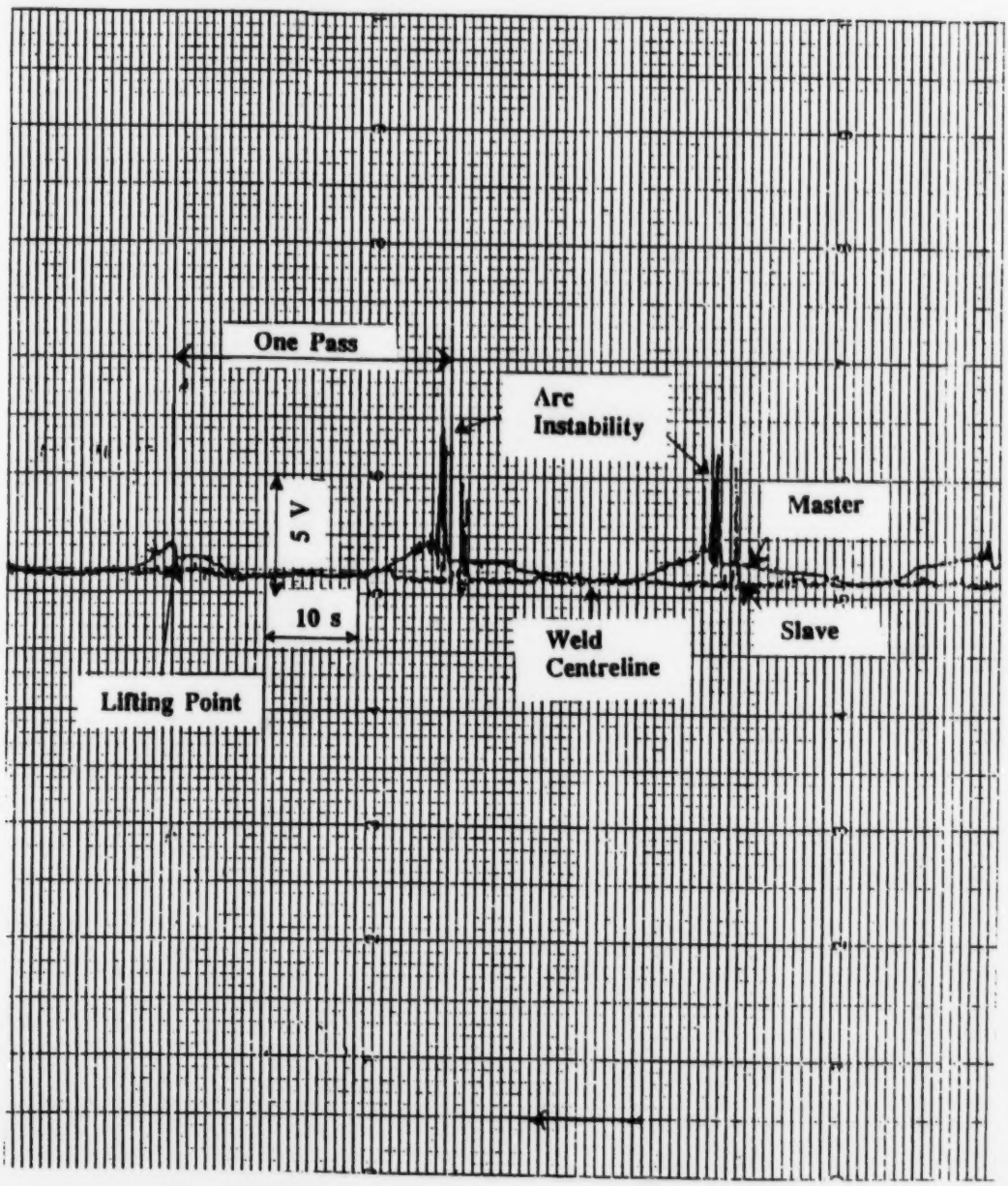

Figure 7. Welding voltage versus time. Arc instability appears at the lifting points.

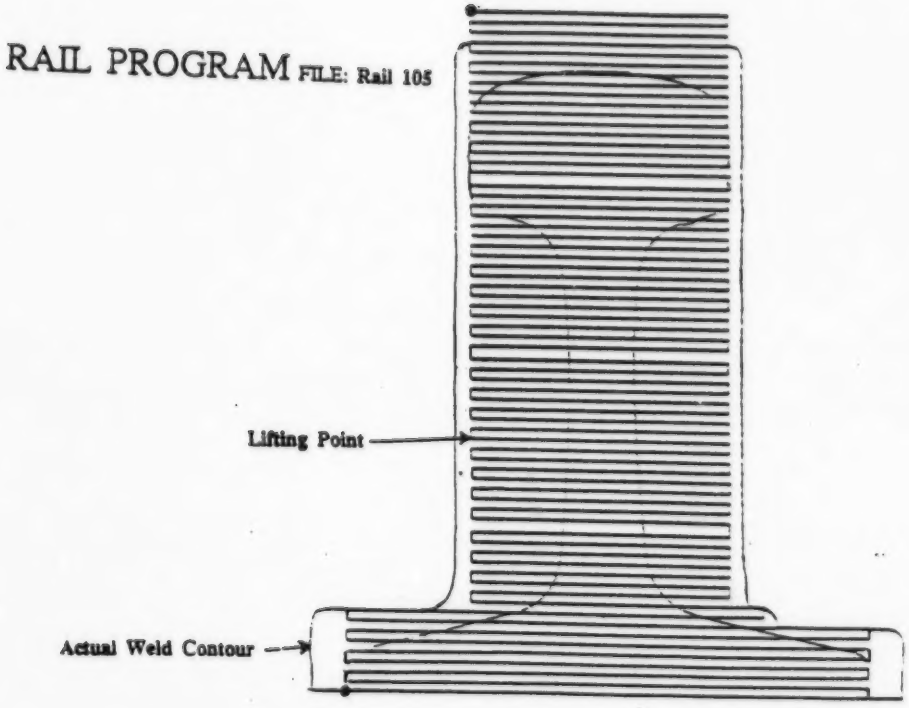

Figure 8. Pattern of the welding head motion.

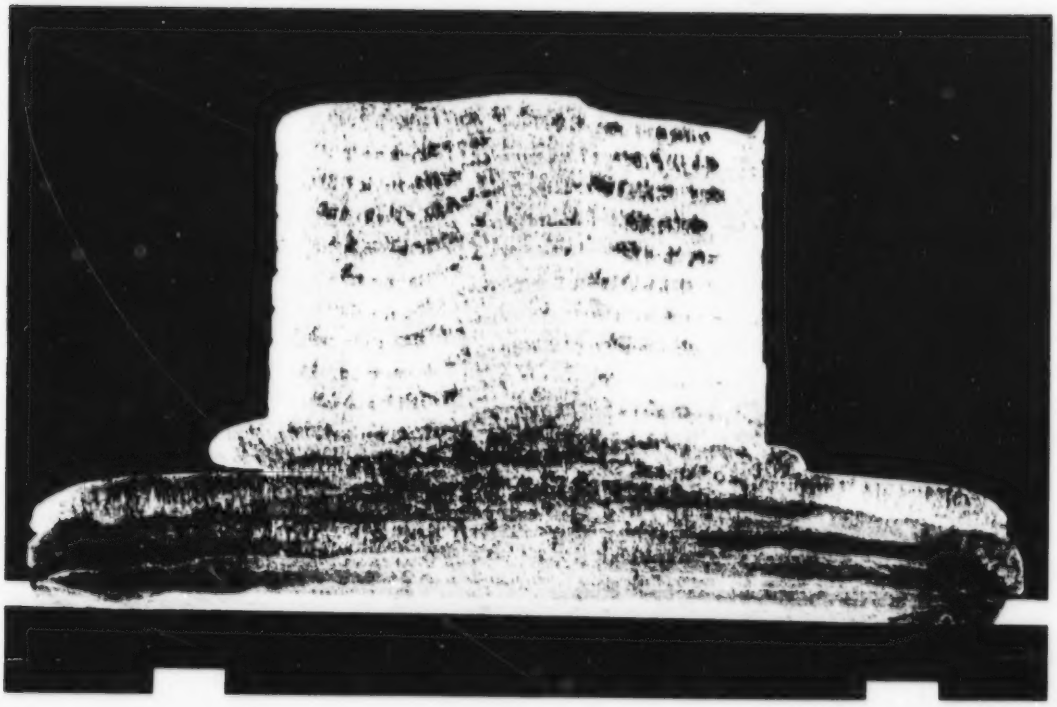

Figure 9. Longitudinal section of the weld showing layers of the deposited weld metal. Porous free weld metal was produced.

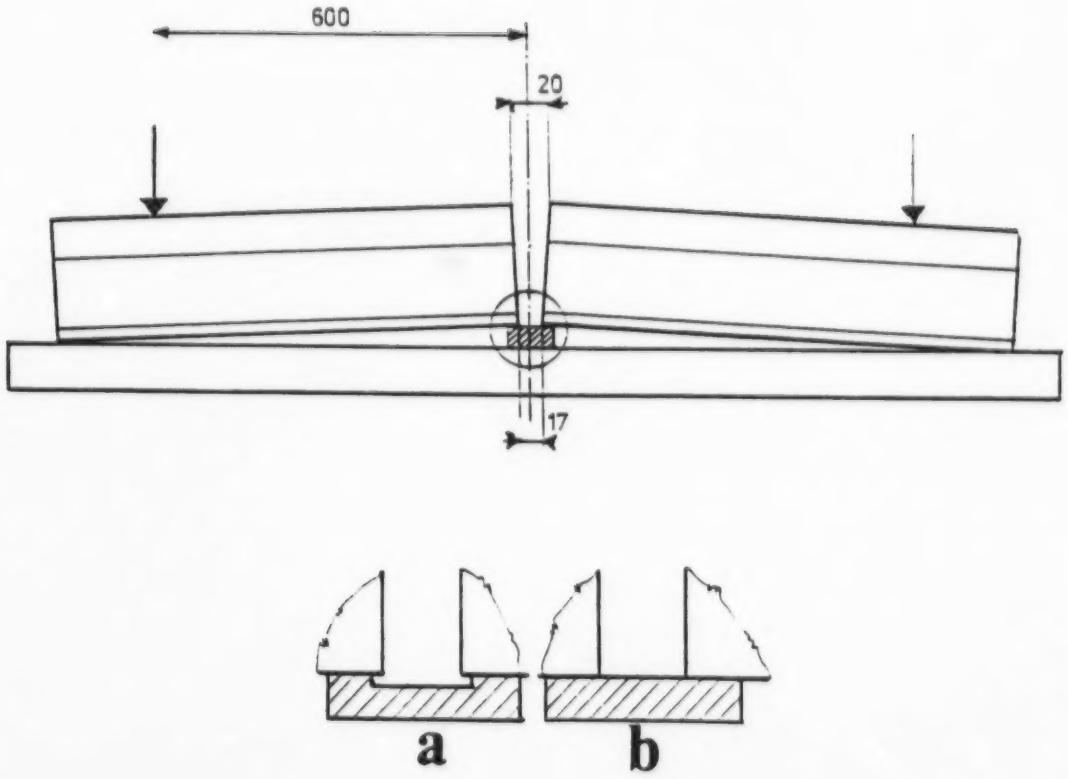

Figure 10. Rail set-up before welding (a) weld backing with grooved bar (b) straight backing.

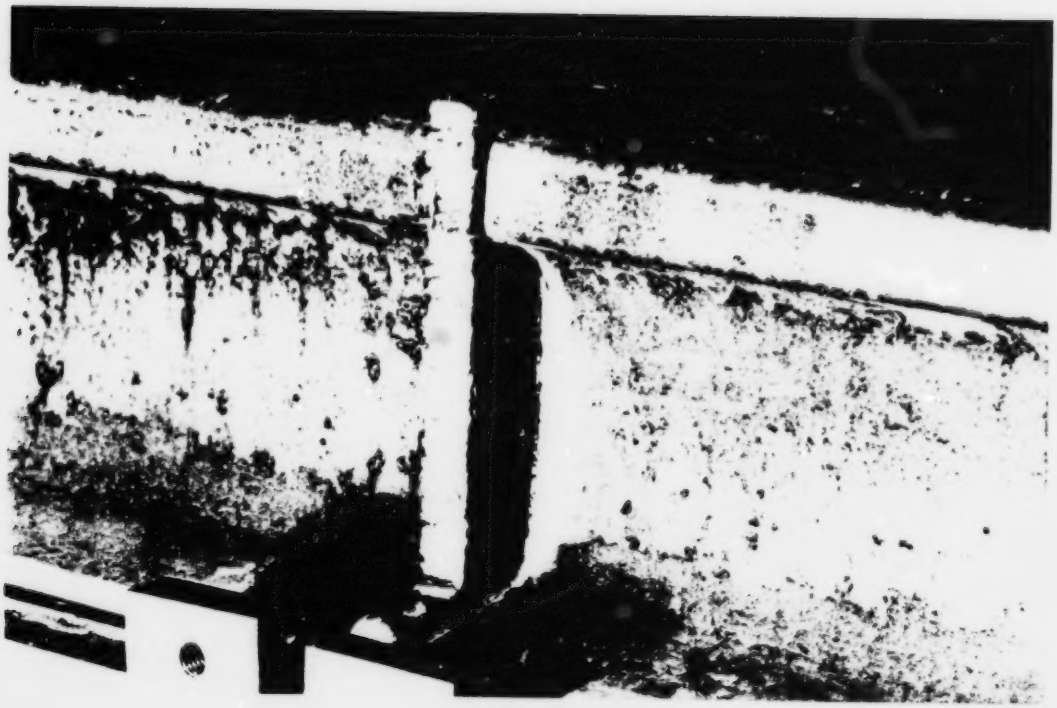

Figure 11. Appearance of the finished weld.

Figure 12. Cross section of the non-stop rail weld. Lack of fusion visible in the rail base as a result of arc instability (#080). Magn. 0.7X

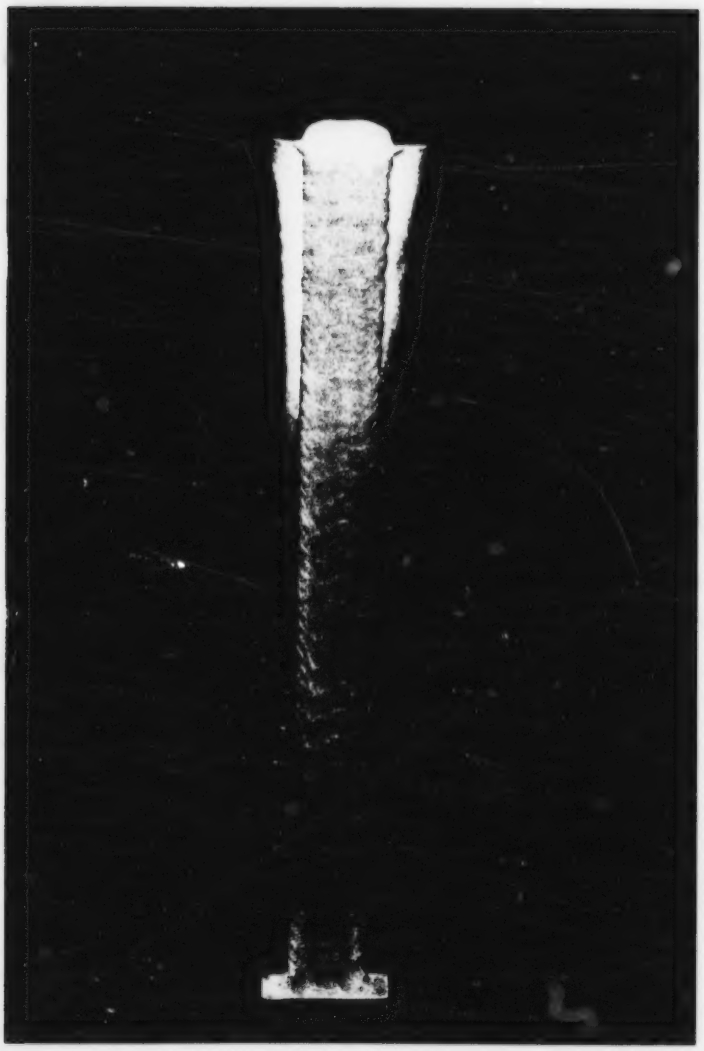

Figure 13. Cross section of the non-stop defect free weld demonstrating unique deposition pattern of the twin wire (#086). Magn. 0.7X

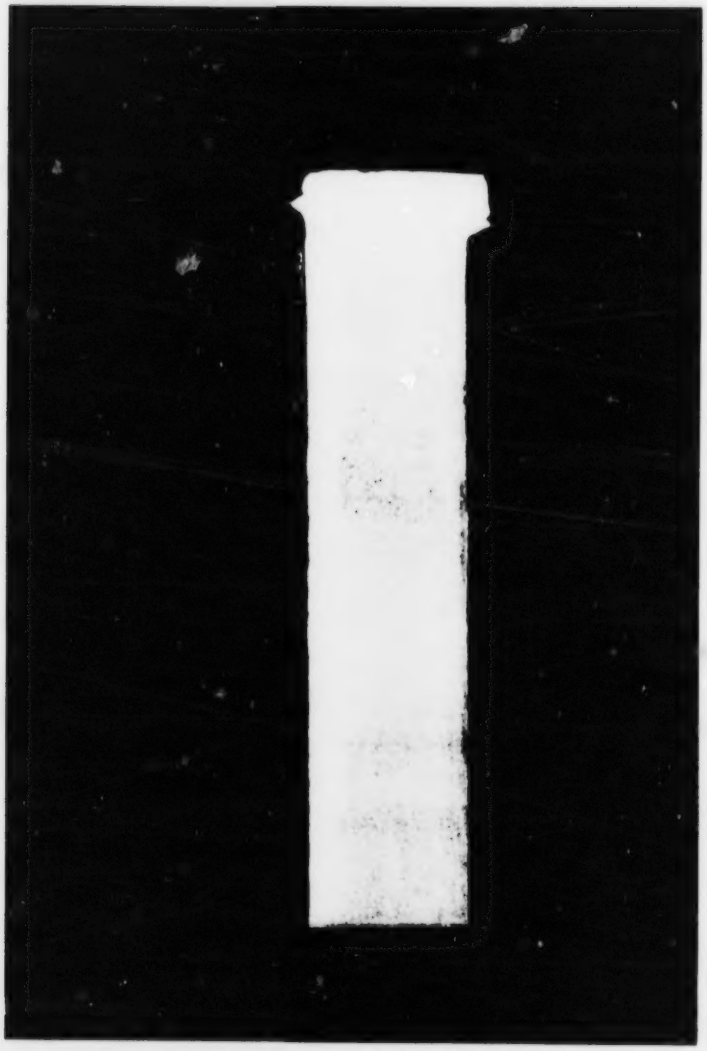

Figure 14. Cross section of the rail base parallel with the base (#070). Magn. 1.35X

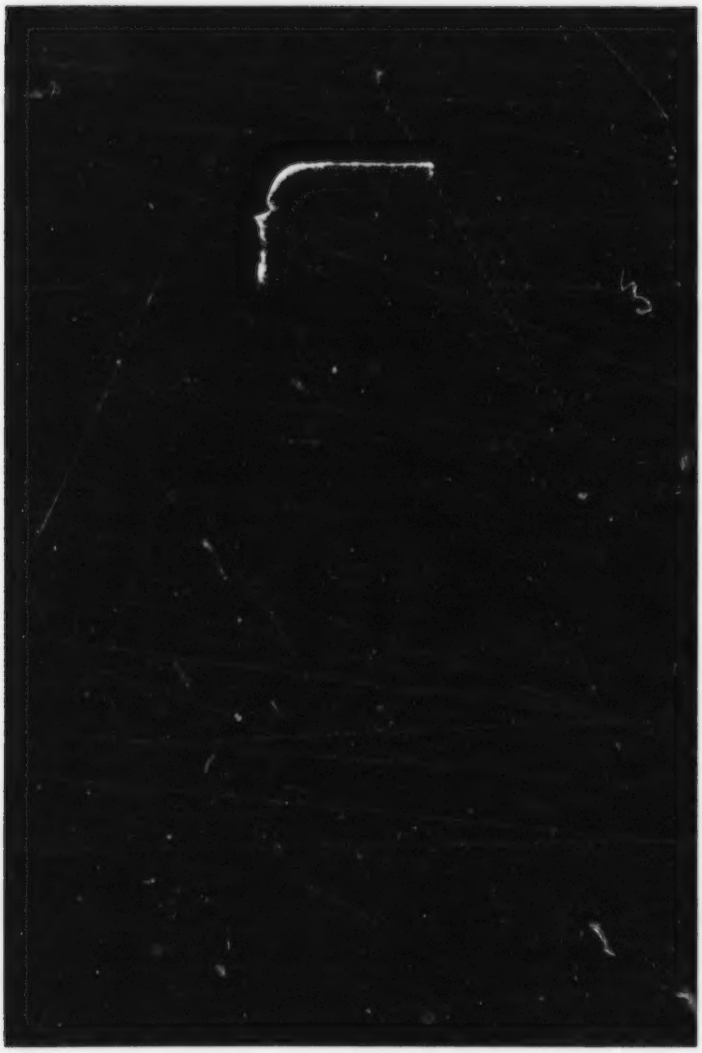

Figure 15. Cross section of the rail head parallel with the base (#085) showing hot cracks. Magn. 1.3X

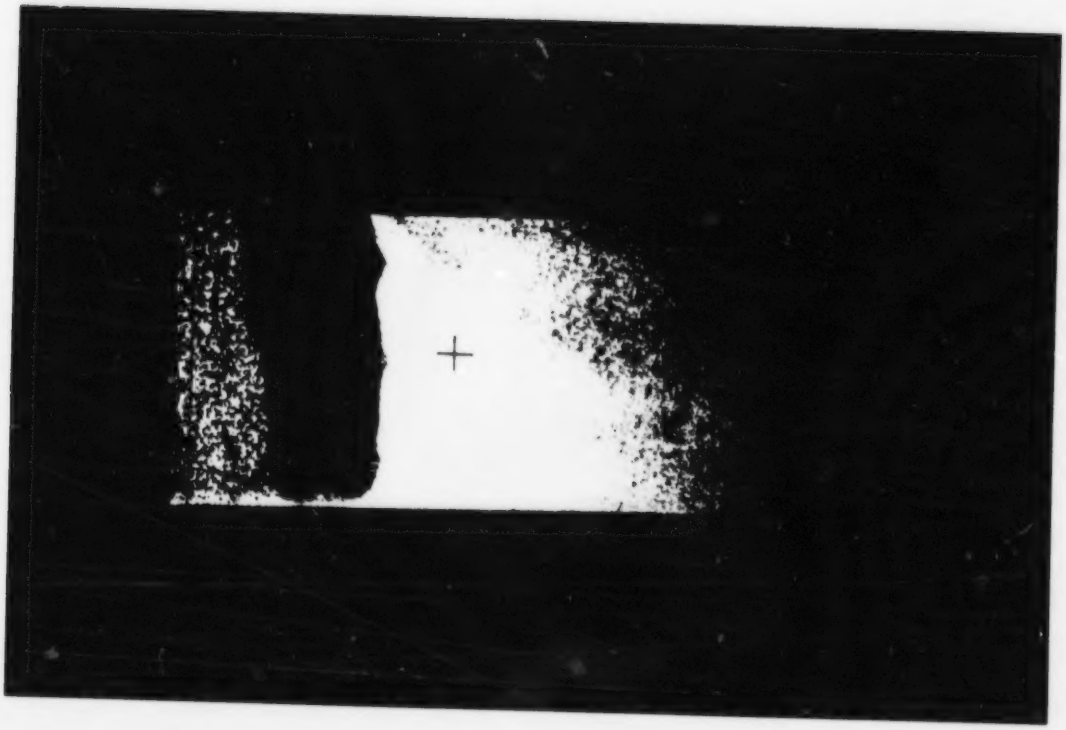

Figure 16. Fine structure in a rail base (#078). Magn. 4.3X
From the left to right: base metal -HAZ- weld metal.

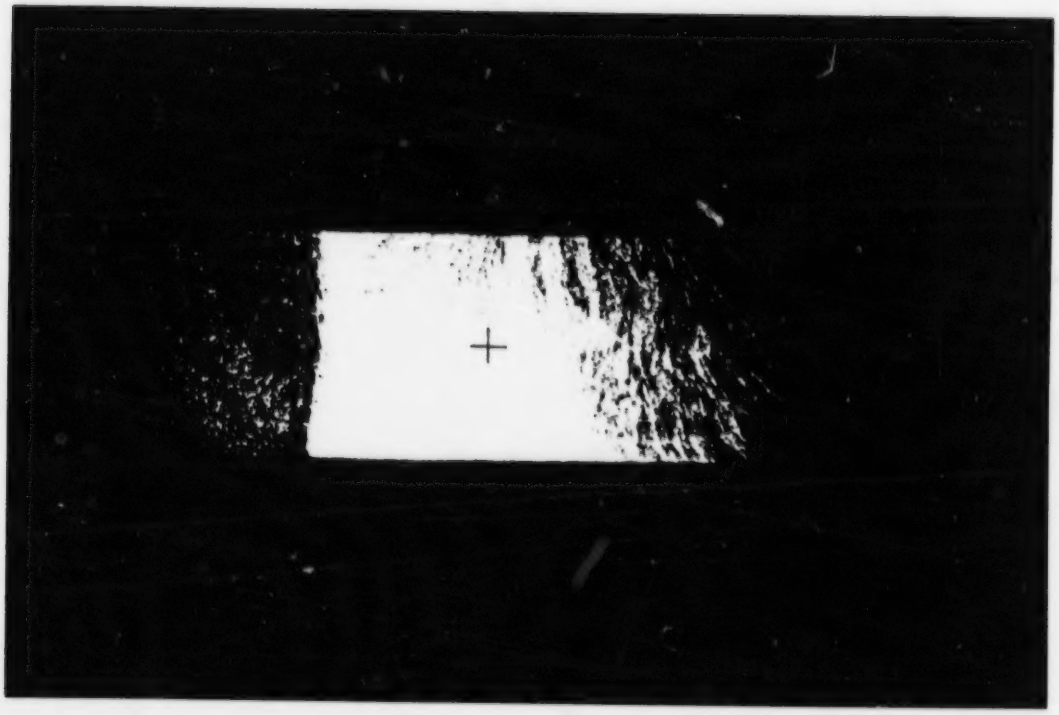

Figure 17. Columnar structure in a rail weld (#080). Individual passes are hard to identify. Magn. 4.3X
From the left to right: HAZ - weld metal

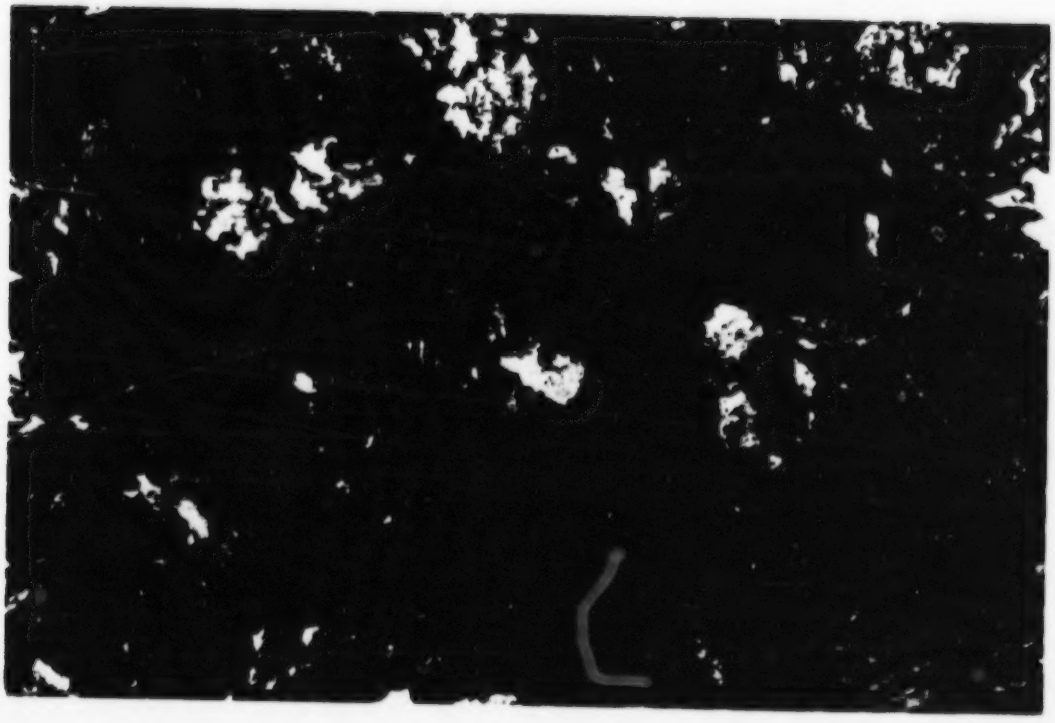

Figure 18. Perlitic structure of the rail parent metal. Microvoids are visible throughout the structure (#078). Magn. 100X

Figure 19. Weld metal microstructure from the upper part of weld (#078). Wire ER 70 S-6. Magn. 100X

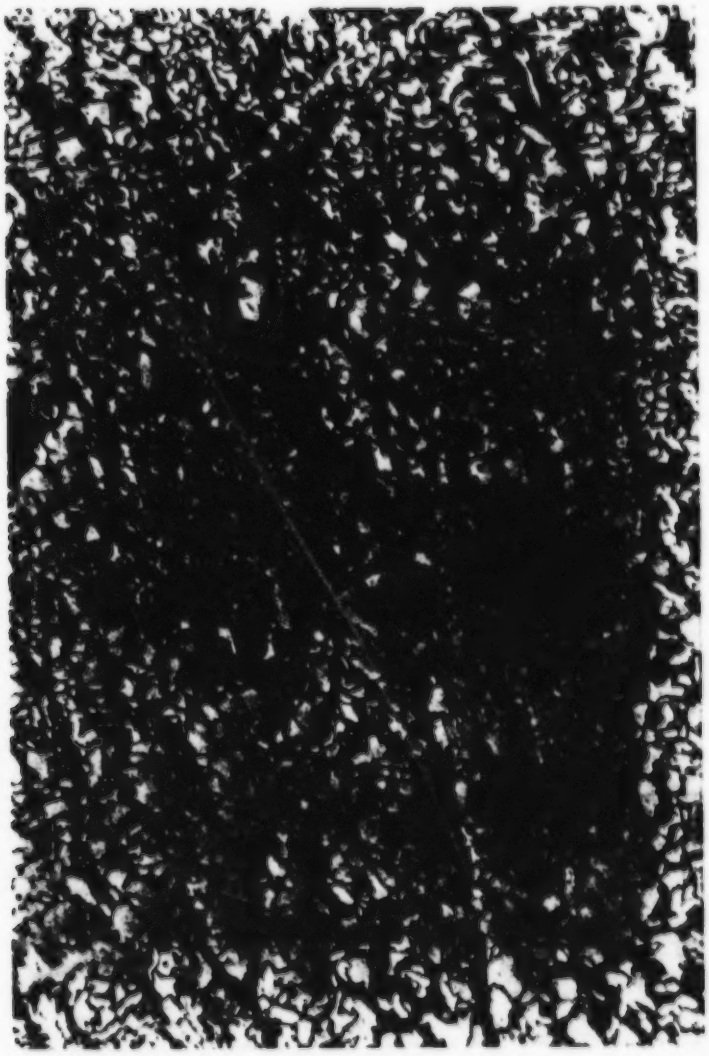

Figure 20. The same weld metal microstructure as Figure 19 (#078) after higher magnification. Magn. 300X. The shrinkage crack is visible in the centre.

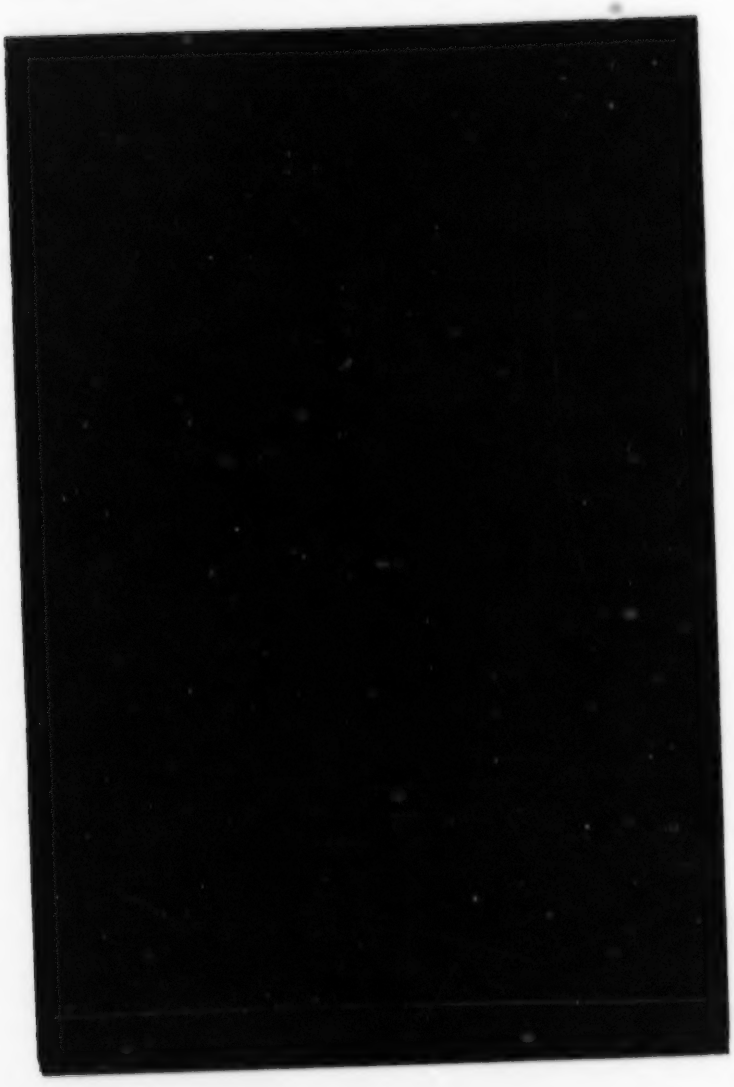

Figure 21. Weld metal microstructure (#081). The shrinkage crack is also visible between dendrites of the high tensile weld deposit ER 120 S-1. Magn. 200X.

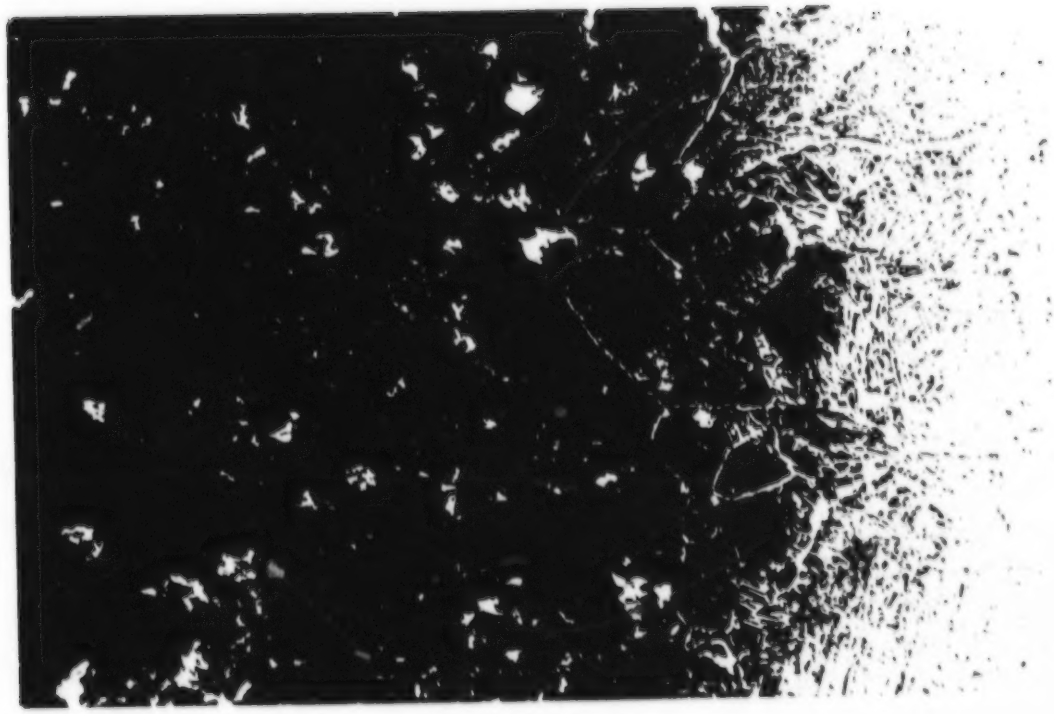

Figure 22. Fusion line between parent and weld metal in an upper portion of the weld. Typical liquation cavities are visible (#078). Magn. 100X.

Figure 23. Fusion line between parent and weld metal in a rail base. In spite of higher magnification (200X) no enlarged microvoids were found (#078).

Figure 24. Fusion line between rail and weld metal in an upper portion of the weld. Typical liquation cavities are visible also in Algoma rail (#081). Magn. 200X.

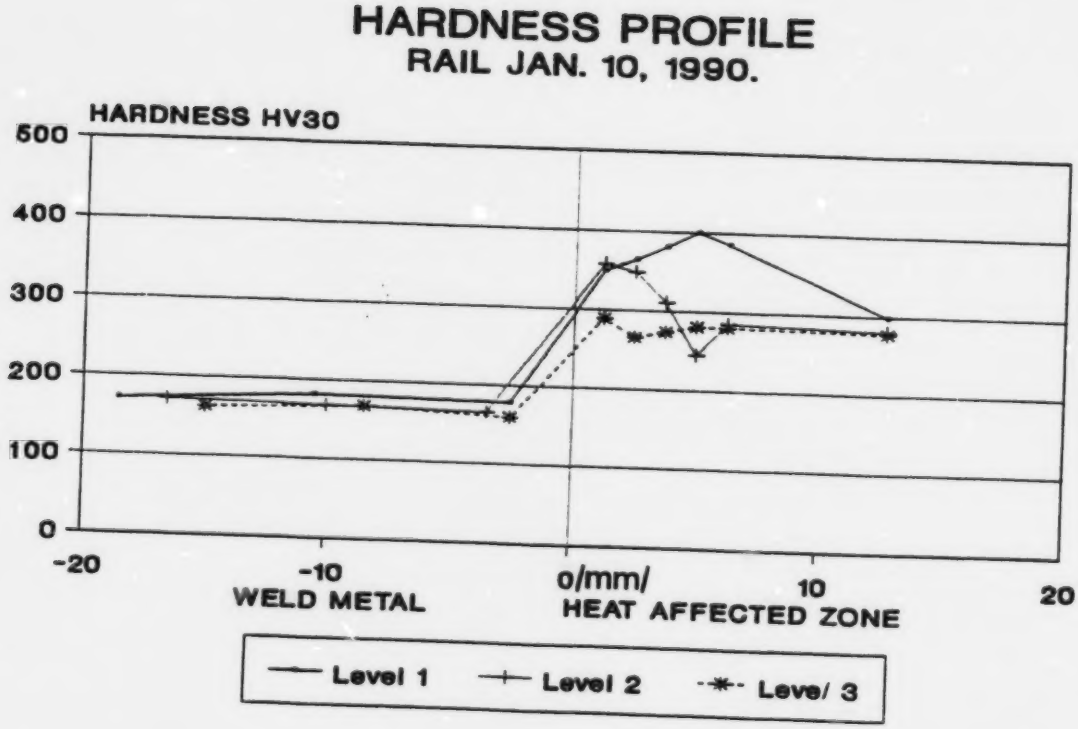

Figure 25. Hardness profile (#073)
(Fusion line at 0 mm)

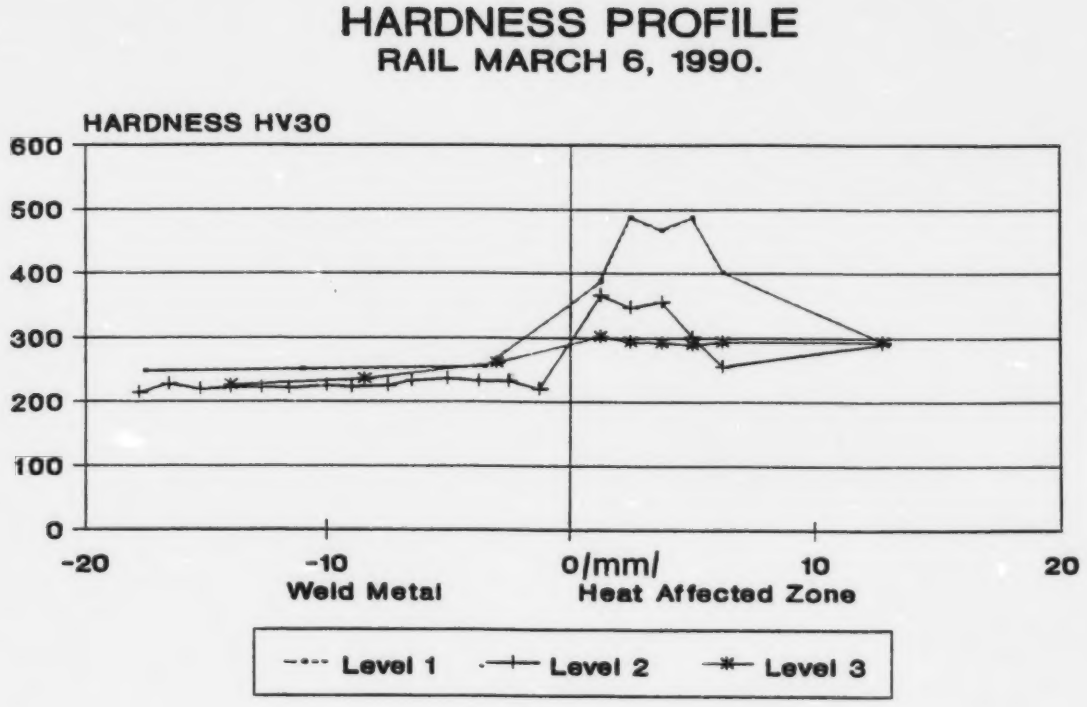

Figure 26. Hardness profile rail (#080)
(Fusion line at 0 mm)

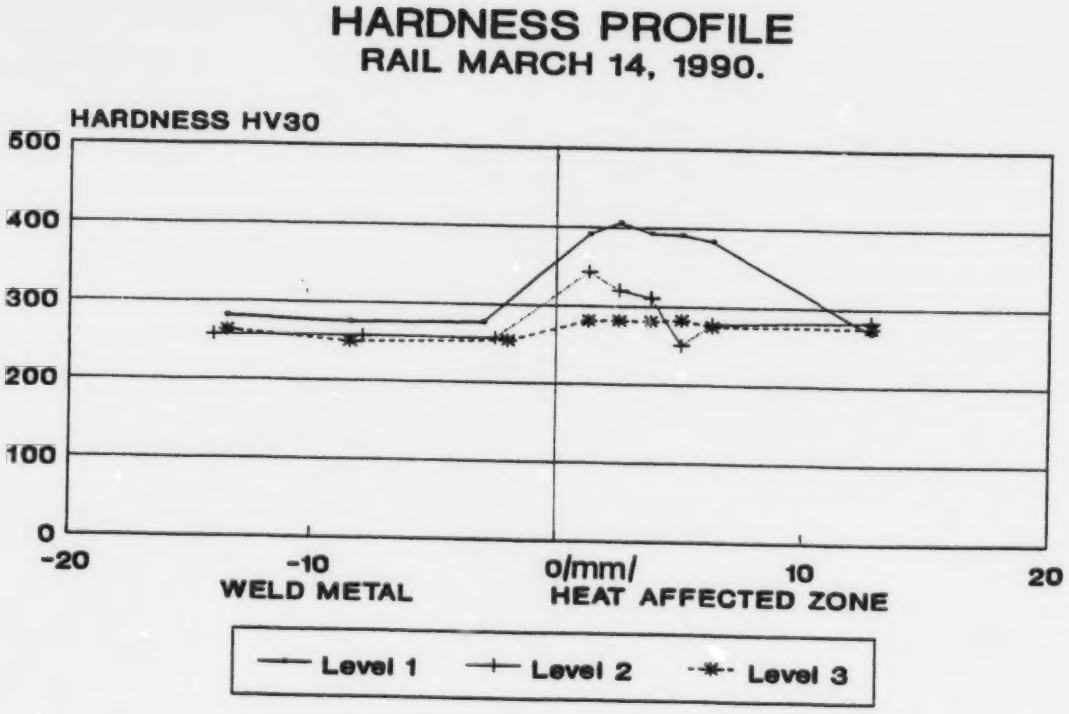

Figure 27. Hardness profile rail (#081)
(Fusion line at 0 mm)

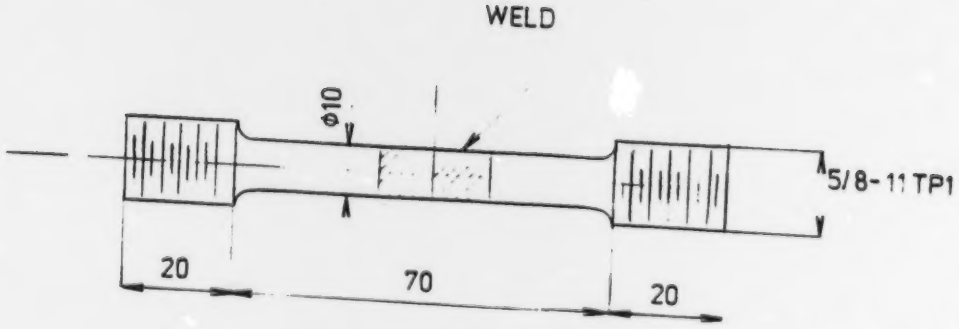

Figure 28. Metric round tensile specimen.

Figure 29. Fracture surface in a tensile specimen showing presence of shrinkage cavities in the weld metal. Magn. 6X

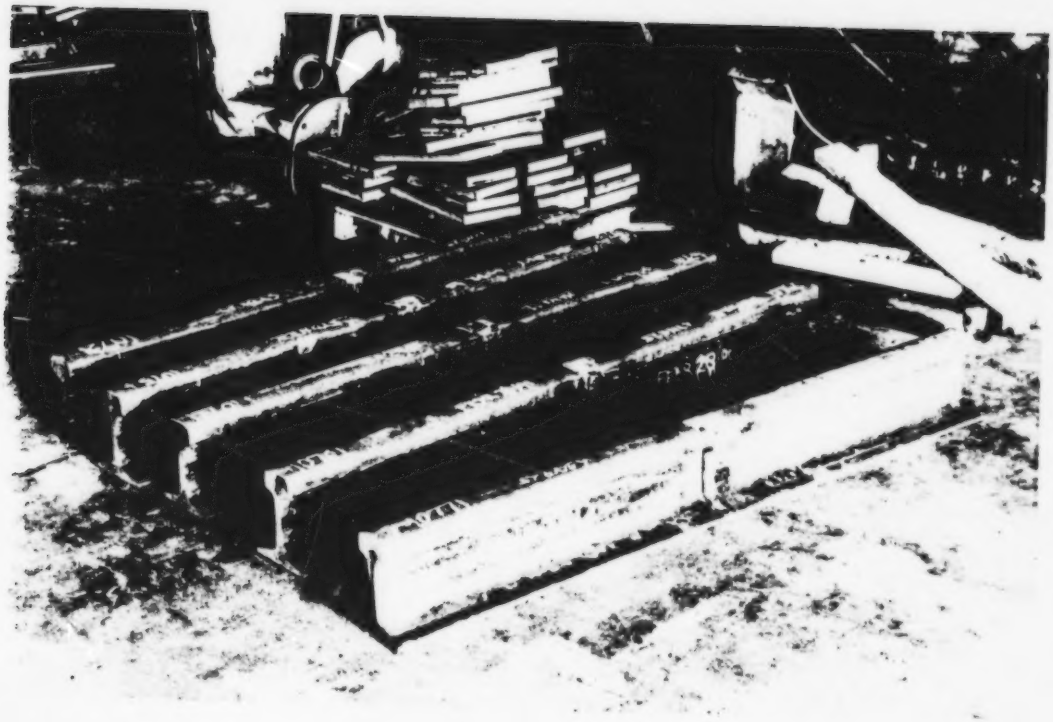

Figure 30. Welded sections before slow bend testing.

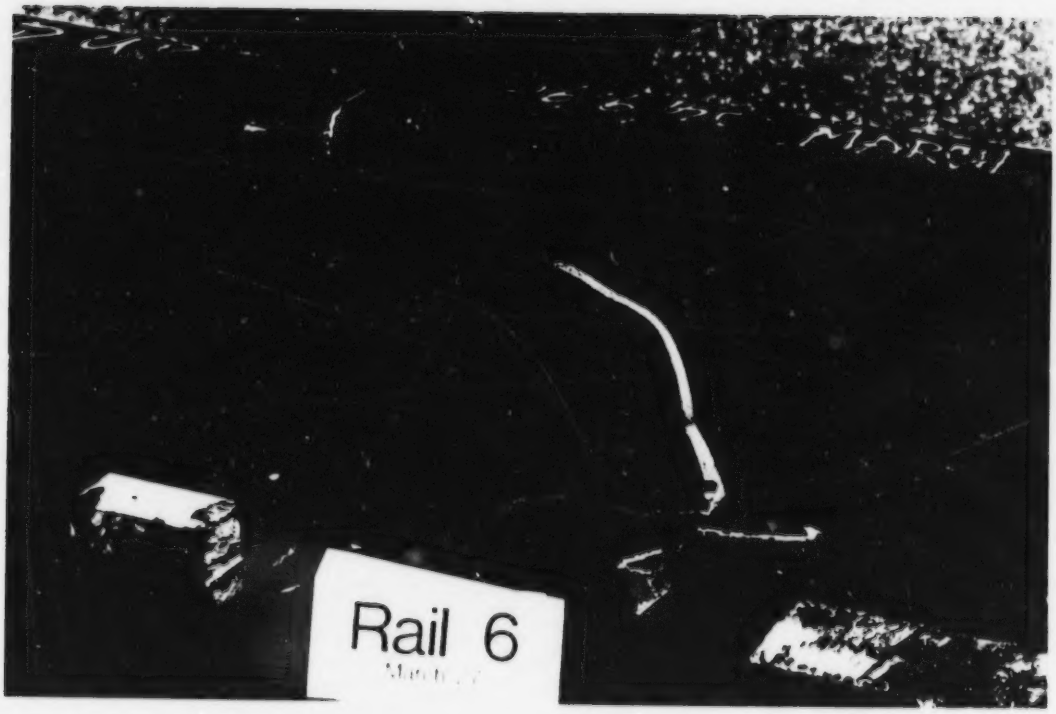

Figure 31. Fracture surface (base in tension) after bend test, showing a second fracture (#082).

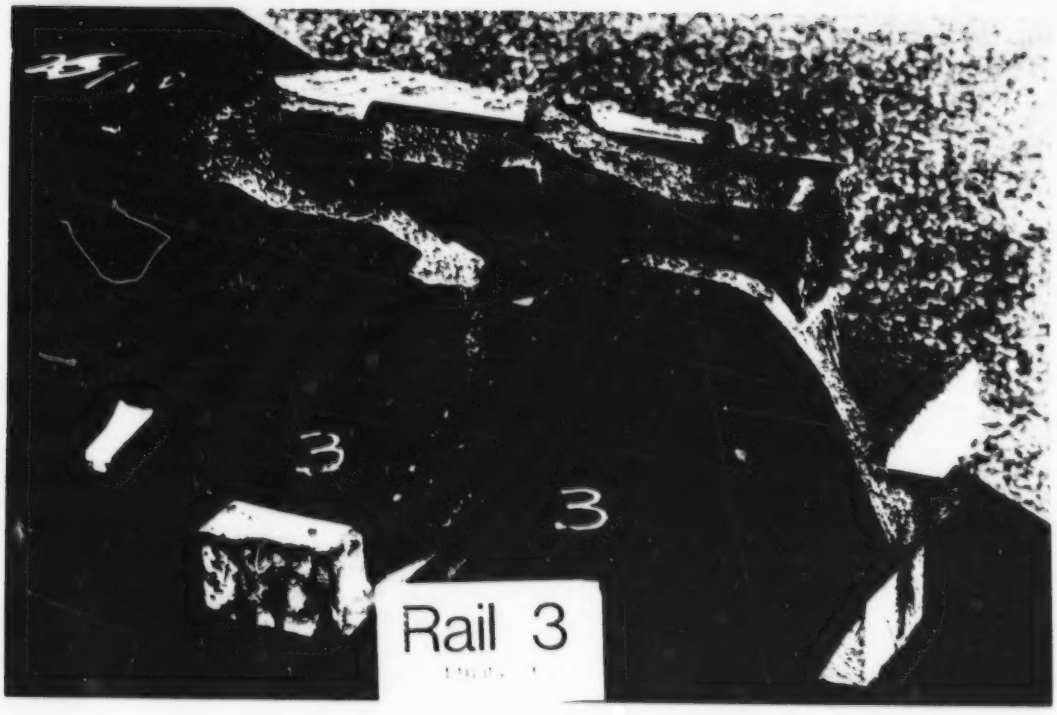

Figure 32. Fracture surface (base in tension) after bend test demonstrating similar character as the rail 6 (#076).

Figure 33. Fracture surface (base in tension) after bend test with non-typical character (#074).

Figure 34. Fracture surface (base in tension) after bend test with the highest deflection (#083).

Figure 35. Fracture (head in tension) after bend test showing coarse structure in a rail weld metal as the result of shrinkage cavities (#077).

Figure 36. Fracture (head in tension) after bend test showing coarse structure in the most of the rail weld metal (#079).

Figure 37. Fracture (head in tension) after bend test demonstrating propagation from the HAZ in the rail head (#084).

Table 1

Optimum Welding Conditions

Power Source	Synchronized pulsed frequency modulated twin wire, inverter type air cooled, maximum average current 200A, 60% duty cycle (WIC development)
Head	Twin wire GMAW-Narrow Gap, triple shielding, maximum average current 200A, 100% duty cycle, liquid cooled body and nozzle, 13 min wide (WIC development)
Feeders	Standard 4 rolls Hobart
Manipulation	Computer controlled motorized X-Y sides Techno (WIC adaption)
Rail Clamping and Cooling System	Rigid jig and copper chill blocks (4 pieces) with internal cooling (WIC development)
Rail	AREA 136 lbs (any grade)
Rail gap	Base 17 mm, head 20 mm
Rail backing	Steel bar 30 x 6 x 200 mm with recess 2 mm deep
Preheat	100°C
Consumables	Solid wire diameter 0.9 mm (0.035") (ER70, ER100, ER120)
Electrode Stick-out	15 min
Horizontal Distance Between Wires (at indicated stickout)	9 mm
Shielding Gas	90%Ar+10%CO_2
Gas Flow Central Tube	15 CFH
Gas Flow Sides	30 CFH
Welding Current Peak	280A master, 300A slave
Welding Current Background	40 A master, 50A slave
Pulse Duration	4.5 ms master, 5.0 ms slave
Average Welding Voltage	25-27V
Wire Feed Speed	8.89 m/min (350 in/min)
Travel Speed	127 mm/min (5 in/min)
Lifting Distance	3 mm
Lifting Speed	540 mm/min (21.25 in/min)
Welding Head Cooling Rate	4l/min (1 gal/min)
Chill Blocks Cooling Rate	10l/min (2.5 gal/min)

TABLE 2

Rail Welds Identification and Summary of the Testing and Welding Matrix

Identification #	Weld Rail #	Testing	Rail Manufact.	Wire
070		H	Sydney	ER 70 S-6
073		H	Sydney	ER 70 S-6
074	1	B1	Sydney	ER 70 S-6
075	2	B2	Sydney	ER 70 S-6
076	3	B3	Sydney	ER 70 S-6
077	4	B4	Sydney	ER 70 S-6
078		H M	Sydney	RB ER 70 S-6 RB ER 120 S-1
079	5	B5	Sydney	ER 70 S-6
080		H M	Sydney	WIRE 1 ER 70 S-6 WIRE 2 ER 120 S-1
081		H M	Algoma	ER 120 S-1
082	6	B6	Algoma	ER 120 S-1
083	7	B7	Algoma	ER 120 S-1
084	8	B8	Algoma	ER 120 S-1
085		T	Algoma	ER 120 S-1
086		H	Algoma	ER 120 S-1
087			Algoma	ER 120 S-1

*** TESTING METHODS:**

M - Metallography

H - Hardness Profile

T - Tensile

B - Slow Bend Test

Table 3
Tensile Test Report

TENSILE TEST REPORT

Client:
Client P.O. Number:
NC Contract Number: AC-350
Test Standard:

Specimen Standard:
Specimen Type: ROUND
Specimen Material: RAIL STEEL
Specimens Obtained By: ANSC

Specimen Number	#5	#6	#8	#9	#10
Initial Thickness or Diameter (mm in.)	0.394(4)	0.395(1)	0.394(4)	0.394(6)	0.394(7)
Initial Width (mm in.)					
Initial Cross-sectional Area (mm² in²)	0.122(2)	0.122(6)	0.122(2)	0.121(9)	0.122(4)
Initial Gauge Length (mm in.)					
Final Thickness or Diameter (mm in.)					
Final Width (mm in.)					
Final Cross-sectional Area (mm² in.²)					
Final Gauge Length (mm in.)					
Yield or Offset Load* (kN lb)					
Maximum Load (~~kN~~ lb)	14,275	11,914	4,335	3,660	4,106
Yield Stress (MPa psi)					
Ultimate Tensile Strength (MPa psi)	117,000	97,200	117,000	1,200	5,000
Elongation (%)					
Reduction of Area (%)					
Failure Location					

* Percentage of offset used to determine offset load: 0.1, 0.2, 0.5

Comments

Date: 3 Th March 92
Tested By: Jan Montgomery
Witnessed By: [illegible]
Project Engineer: [illegible]

Table 4
Slow Bend Test

CN RAIL

Canadian National Railways
Technical Research Centre
3950 Hickmore Avenue
St-Laurent, Québec
H4T 1K2

FK 4015-050AA-1

14 May 1990

Dr. P. Somsky
Group Leader
Fabrication Technology
Welding Institute of Canada
391 Burnhamthorpe Road East
Oakville, Ontario
L6J 1G3

Dear Sir:

RE: SLOW BEND TESTS - YOUR RAIL WELDING PROJECT RC350

We have completed the slow bend testing of eight welded rail sections that were submitted to our laboratory in connection with your letters of March 13 and April 2, 1990. The test results are summarized in the following table:

SAMPLE ID	POSITION	LOAD (lbs.)	DEFLECTION (in.)
Rail 1	Base in tension	366,000	0.50"
Rail 2	Base in tension	432,000	0.70"
Rail 3	Base in tension	414,000	0.70"
Rail 4	Head in tension	390,000	0.75"
Rail 5	Head in tension	348,000	0.45"
Rail 6	Base in tension	456,000	0.75"
Rail 7	Base in tension	390,000	1.05"
Rail 8	Head in tension	342,000	0.30"

.../2

Appendix 1

THYSSEN NiMoCr ER 100 S–1

THYSSEN

Bare solid electrode for GMAW acc. to AWS A 5.28

Appendix 1

TYPICAL WIRE ANALYSIS %

C	Si	Mn	P	S	Mo	Ni	Cr
.09	.50	1.70	.010	.010	.50	1.45	.20

MECHANICAL PROPERTIES OF THE ALL WELD METAL (AS WELDED)
Shielding Gas: CO_2

Tensile Strength		Yield Strength		Elongation in 2 inch, %	Typical Charpy Impact Strength			
psi	MPa	psi	MPa		°F	°C	ft lb	Joule
≥ 107000	≥ 740	≥ 98000	≥ 680	≥ 18	+68	+20	70	90
					–40	–40	30	40

MECHANICAL PROPERTIES OF THE ALL WELD METAL (AS WELDED)
Shielding Gas: Argon / CO_2

Tensile Strength		Yield Strength		Elongation in 2 inch, %	Typical Charpy Impact Strength			
psi	MPa	psi	MPa		°F	°C	ft lb	Joule
≥ 113000	≥ 780	≥ 105000	≥ 720	≥ 17	+68	+20	80	100
					–80	–62	30	40

Appendix 2

October 18, 1989

Welding Institute of Canada
391 Burnhamthorpe Road East
Oakville, Ontario
L6V 6C9

CERTIFICATE OF CHEMICAL ANALYSIS

Purchase Order No.:	RD5645	Part No.:	2402F25
L-Tec S.O. No.:	055155	Part Description:	L-Tec 120 Wire
Quantity:	32 kg.	0.9 mm Diameter	

This is to certify that this material will conform to AWS A5.28, ASME SFA5.28. It has the following chemical analysis meeting the requiremnts of classification ER120S-1.

Heat No.	120025
C.	.06
Mn.	1.63
P.	.006
S.	.005
Si.	.38
Cu.	.01
Ni.	2.37
Cr.	.31
Mo.	.50
Al.	.012
Ti.	.010
Zr.	.015
V.	.001

Stephen Rudd
Welding Technician

:jc
(0305U)